



The 13th European Radar Conference

## Radar Performance in Clutter - Modelling, Simulation and Target Detection Methods

WF02

Simon Watts, UCL

Keith Ward, Igence Radar

Maria Greco, University of Pisa

Slide 1  
of 198



The 13th European Radar Conference

## Radar Clutter Modelling

Simon Watts

UCL

[simon.watts@ucl.ac.uk](mailto:simon.watts@ucl.ac.uk)

Slide 2  
of 198



## Introduction to Radar Clutter

Slide 3  
of 198



## Radar Clutter

Radar signals are comprised of

- Targets
- Thermal noise
- Clutter

Clutter is defined as unwanted returns from

- Land
- Sea
- Rain
- Birds etc.

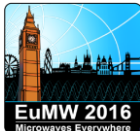
Clutter is further subdivided into discrete and distributed multiple scatterers



Sources of clutter

[Images from *Representing Clutter*, Chapter 25 of "Stimson's Introduction to Airborne Radar", 3<sup>rd</sup> Edition, SciTech Publishing, May 2014 (H.D.Griffiths, C.J.Baker and D. Adamy, Eds.) ]

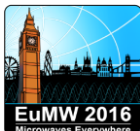
Slide 4  
of 198



## Clutter Models

- Clutter is often characterised by mathematical models
- Models of clutter are required for:
  - Performance prediction
  - Simulation
  - Comparative performance assessment
  - Design of detection processing
  - Measurement of performance for acceptance
- Models may be theoretical or empirical and usually represent typical or average performance
- Real life on any given trial may “deviate” considerably from the models

Slide 5  
of 198



## Distributed Clutter

### Key Characteristics

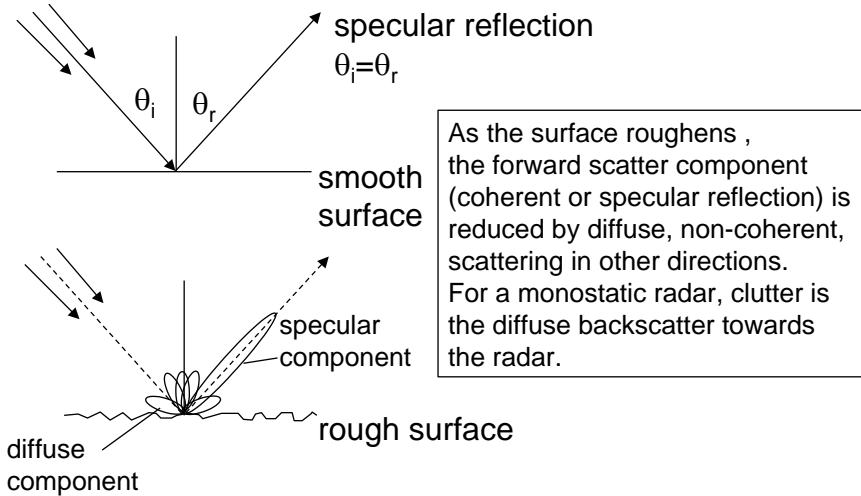
- Reflectivity
- Polarisation scattering matrix
- Amplitude Statistics
- Spectrum
- Spatial Correlation

Theoretical and empirical models used for radar design

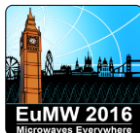
Slide 6  
of 198



## Surface Scattering



Slide 7  
of 198



## Reflectivity

- Clutter is often approximated to comprise of multiple scatterers distributed uniformly over the radar resolution cell.
- Effective radar cross-section of clutter return depends on area of the radar patch

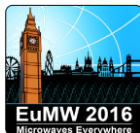
Surface scattering is defined by area reflectivity  $\sigma^0$ :

$$\sigma^0 = \sigma / A \quad \text{dBm}^2 / \text{m}^2$$

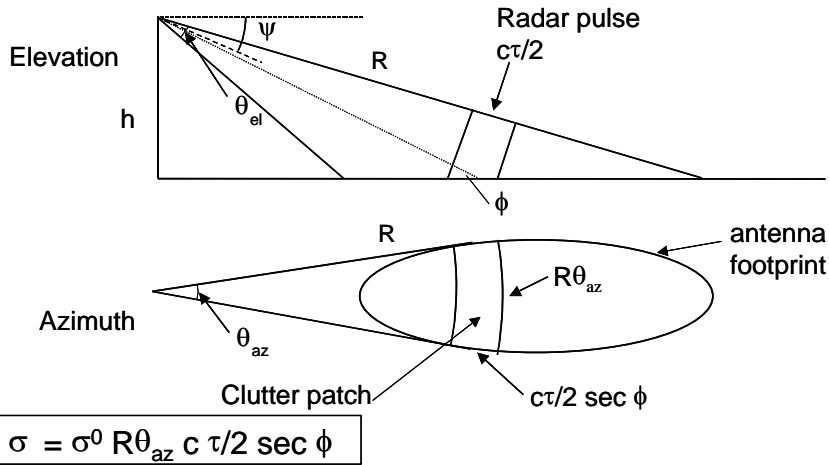
Volume scattering is defined by volume reflectivity  $\eta$ :

$$\eta = \sigma / V \quad \text{dBm}^2 / \text{m}^3$$

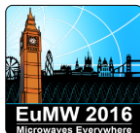
Slide 8  
of 198



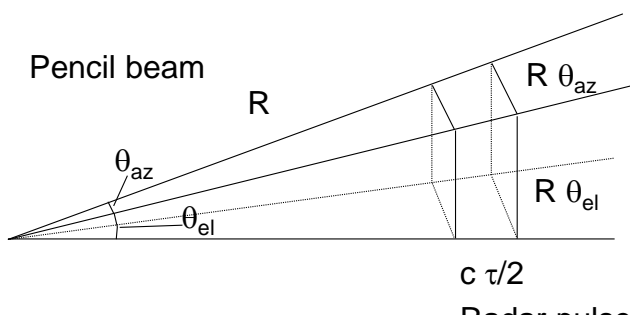
## Surface Clutter



Slide 9  
of 198



## Volume Clutter



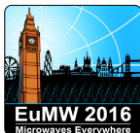
Slide 10  
of 198



# Polarisation

- A wave in which the direction of the electric and magnetic field vectors, **E** and **H** respectively, reside in fixed planes as the wave progresses is said to be polarised.
- The plane in which the **E** vector moves is called the plane of polarisation. The polarisation scattering matrix, **S**, describes the amplitude and relative phase of returns from different combinations of polarisations on transmit and receive.
- It is observed that many clutter characteristics are very dependent on the polarisation of the radar signal and so an understanding of polarisation is important.

Slide 11  
of 198



# Polarisation Scattering Matrix

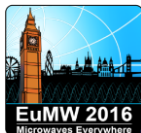
$$\mathbf{S} = \begin{vmatrix} \sqrt{\sigma_{HH}} e^{j\rho_{HH}} & \sqrt{\sigma_{HV}} e^{j\rho_{VH}} \\ \sqrt{\sigma_{VH}} e^{j\rho_{HV}} & \sqrt{\sigma_{VV}} e^{j\rho_{VV}} \end{vmatrix}$$

$$\left. \begin{array}{l} \sigma_{HV} = \sigma_{VH} \\ \rho_{HV} = \rho_{VH} \end{array} \right\} \text{for backscatter}$$

$$\begin{bmatrix} E_H \\ E_V \end{bmatrix}_{receive} = A \mathbf{S} \begin{bmatrix} E_H \\ E_V \end{bmatrix}_{transmit}$$

$\sigma_{HH}$  rcs for Tx on H and Rx on H polarisation  
 $\sigma_{VV}$  rcs for Tx on V and Rx on V polarisation  
 $\sigma_{VH}$  rcs for Tx on V and Rx on H polarisation

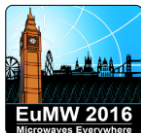
Slide 12  
of 198



# Polarisation Scattering Matrix

	<b>S</b>		<b>S</b>
Sphere	$\begin{bmatrix} 1 & 0 \\ 0 & 1 \end{bmatrix}$	Dihedral at angle $\psi$	$\begin{bmatrix} \cos 2\psi & \sin 2\psi \\ \sin 2\psi & -\cos 2\psi \end{bmatrix}$
Dihedral at 0 deg	$\begin{bmatrix} 1 & 0 \\ 0 & -1 \end{bmatrix}$	Linear Target at angle $\psi$	$\begin{bmatrix} \cos^2 \psi & \frac{1}{2} \sin 2\psi \\ \frac{1}{2} \sin 2\psi & \sin^2 \psi \end{bmatrix}$
Linear Target (Horizontal)	$\begin{bmatrix} 1 & 0 \\ 0 & 0 \end{bmatrix}$	Left hand helix	$\begin{bmatrix} 1 & j \\ j & -1 \end{bmatrix}$
		Right hand helix	$\begin{bmatrix} 1 & -j \\ -j & -1 \end{bmatrix}$

Slide 13  
of 198



# Circular Polarisation

- If the V and H components of the electric field are in phase, linear polarisation is obtained. In general, an arbitrary phase between the V and H fields produces an elliptical polarisation. The special case of a  $\pi/2$  phase shift gives circular polarisation.
- Left-hand circular polarisation  $E_V = jE_H$
- Right-hand polarisation  $E_V = -jE_H$ .

Slide 14  
of 198



## Circular polarisation

Define the circular-polarisation scattering matrix as

$$\begin{bmatrix} E_L \\ E_R \end{bmatrix}_{receive} = \begin{bmatrix} c_{LL} & c_{RL} \\ c_{RL} & c_{RR} \end{bmatrix} \begin{bmatrix} E_L \\ E_R \end{bmatrix}_{transmit}$$

if the linear-polarisation has a scattering matrix given by

$$\begin{bmatrix} E_H \\ E_V \end{bmatrix}_{receive} = \begin{bmatrix} a_{HH} & a_{VH} \\ a_{HV} & a_{VV} \end{bmatrix} \begin{bmatrix} E_H \\ E_V \end{bmatrix}_{transmit}$$

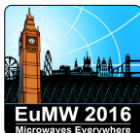
The circular polarisation RCS terms are related to the linear polarisation RCS terms by:

$$\sigma_{LL} = k |c_{LL}|^2 = k \left| \frac{a_{HH} - a_{VV}}{2} + ja_{VH} \right|^2$$

$$\sigma_{LR} = k |c_{LR}|^2 = k \left| \frac{a_{HH} + a_{VV}}{2} \right|^2$$

$$\sigma_{RR} = k |c_{RR}|^2 = k \left| \frac{a_{HH} - a_{VV}}{2} - ja_{VH} \right|^2$$

Slide 15  
of 198



## Use of circular polarisation

- For a sphere, where  $a_{HH} = a_{VV} = 1$  and  $a_{HV} = a_{VH} = 0$  (previous slide),  $\sigma_{LL} = \sigma_{RR} = 0$  and  $\sigma_{LR} = \sigma_{HH} = \sigma_{VV}$ .
- Circular polarisation is used to reduce rain clutter typically reducing reflectivity by about 15dB, to as much as 30dB, dependent on conditions.
- Target signatures may be quite different according to polarisation. Using circular polarisation,  $\sigma_{RL}$  will show odd bounce scatterers whilst  $\sigma_{RR}$  will show even bounce scatterers.

Slide 16  
of 198



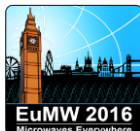
# Amplitude Statistics

- Assume clutter patch has multiple scatterers, rcs  $\sigma_i$ , uniformly spatially distributed, giving random phases  $\theta_i$ .
  - The backscatter voltage is
- $$V = \sum_{i=1}^N \sqrt{\sigma_i} e^{-j\theta_i}$$
- V will be complex and its real and imaginary parts will have Gaussian probability density functions (pdf)

$$p(V) = \frac{1}{\sqrt{2\pi}s} e^{-(V^2/2s^2)}, \quad -\infty \leq V \leq \infty$$

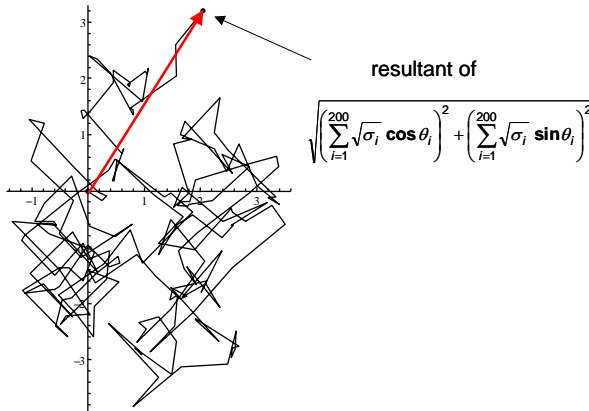
where s is standard deviation of V

Slide 17  
of 198

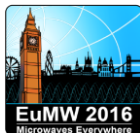


# Gaussian statistics

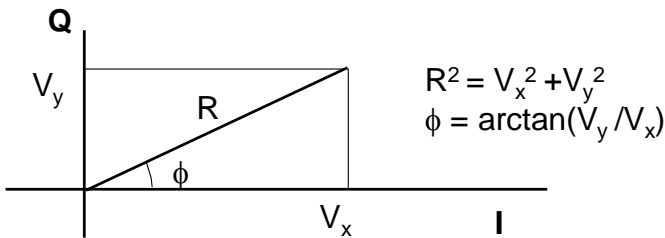
$$V = \sum_{i=1}^N \sqrt{\sigma_i} \exp(j\theta_i)$$



Slide 18  
of 198



## Envelope Amplitude Statistics



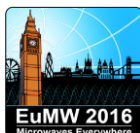
$V_x, V_y$  have Gaussian PDF and phase,  $\phi$ , has uniform PDF;  
 PDF of the envelope  $R$  has a Rayleigh distribution

$$p(R) = \frac{R}{s^2} \exp\left(-\frac{R^2}{2s^2}\right) ; \quad 0 \leq R \leq \infty$$

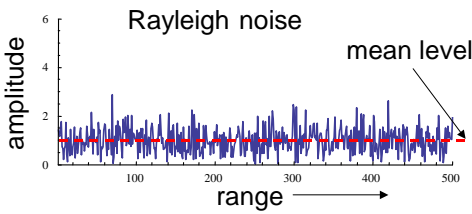
Mean square value of  $R$  is  $2s^2$

This is the power of the envelope and can be related  
 directly to the mean rcs of the clutter (given by  $\sigma^0$ )

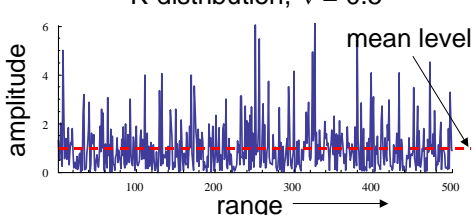
Slide 19  
 of 198



## Non-Gaussian Statistics



- Rayleigh noise and K-distributed clutter ( $\nu=0.5$ ) with mean value 1.
- K-distribution illustrates “spiky” clutter having a “long tailed” amplitude distribution.
- Rayleigh noise derives from standard Gaussian statistics.



Slide 20  
 of 198



## Clutter Spectrum

Movement of scatterers causes a change in phase

$$x(t) = \sum_{i=1}^N \sqrt{\sigma_i} \exp[j\phi_i(t)]$$

*Autocorrelation function*  $R(\tau) = \lim_{T \rightarrow \infty} \frac{1}{2T} \left| \int_{-T}^T x(t)x(t+\tau) dt \right|$

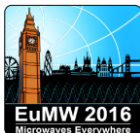
*Power spectral density*  $P(f) = \int_{-\infty}^{\infty} R(\tau) \exp(-j2\pi f \tau) d\tau$

$$R(\tau) = \exp(-\alpha^2 \tau^2) \Leftrightarrow P(f) = \frac{2\sqrt{\pi}}{\alpha} \exp(-\pi^2 f^2 / \alpha^2)$$

**Narrow**  $R(\tau) \rightarrow$  **wide**  $P(f)$

$$R(0) = \int_{-\infty}^{\infty} P(f) df$$

Slide 21  
of 198

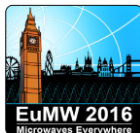


## Clutter Spectra

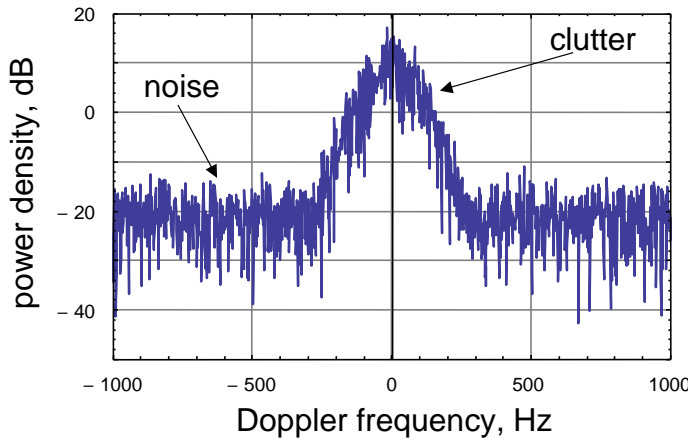
- Clutter spectra are typically approximated by Gaussian shaped psd.
- This may often be a computational convenience rather than a realistic model.
- Typical values of spectral width (standard deviation):
 

Sea	:	1-2 m/s
Land	:	0-1 m/s (for 0-30 m/s wind speed)
Rain	:	2 m/s (typical)
- Mean velocity may not be zero. For sea clutter the mean Doppler is determined by the orbital velocity of wind driven waves. Typical mean clutter velocity is 1/8 wind speed (V pol).

Slide 22  
of 198

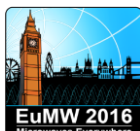


## Doppler spectrum of clutter



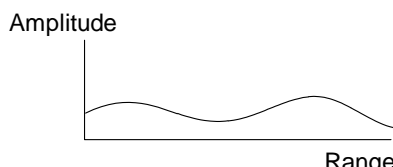
Simulated Gaussian power spectrum with added noise

Slide 23  
of 198

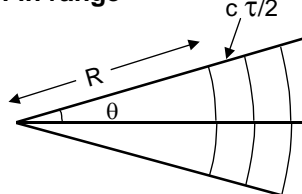


## Spatial Correlation

**Uncorrelated areas in uniform clutter separated by the 3dB azimuth beamwidth,  $\theta$ , or a range resolution cell,  $c \tau/2$ .**

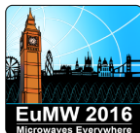


Spatial correlation in range



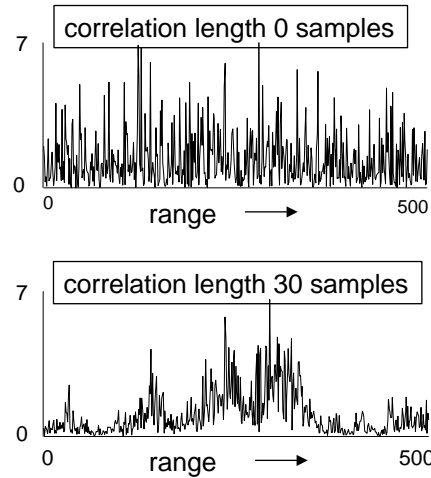
Examples of spatial correlation in clutter

Slide 24  
of 198



## Spatial Correlation

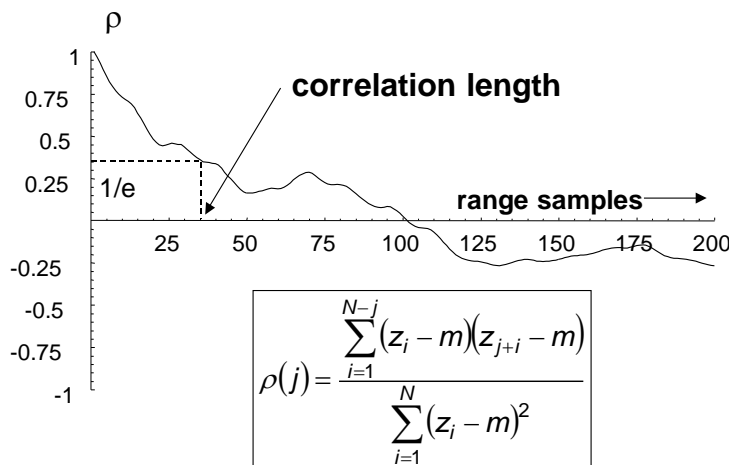
- Clutter returns may exhibit spatial correlation due to underlying structure such as sea swell or undulating hills.
- Illustrations show 500 range samples of K-distributed data with  $\nu=0.5$  and different spatial correlation lengths.



Slide 25  
of 198



## Spatial ACF



Correlation coefficient used to describe spatial correlation

Slide 26  
of 198



## Practical Clutter Models

Rain  
Land  
Sea

Slide 27  
of 198



## Rain Clutter

- Theoretical Characteristics
  - Scattering is assumed to be from multiple spheres; for Rayleigh scattering ( $\pi D / \lambda < 1$ ):

$$\eta = \sum_{i=1}^N \frac{\pi^5 |K|^2 D^6}{\lambda^4}$$

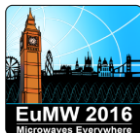
D : drop diameter, N : number of drops

$K \approx 0.93$ , dependent on dielectric constant and  $\lambda$

- For rainfall rate  $r$  mm/hr,

$$Z = \sum_i D^6 \approx 200r^{1.6} \text{ mm}^6/\text{m}^3$$

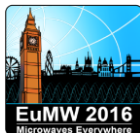
Slide 28  
of 198



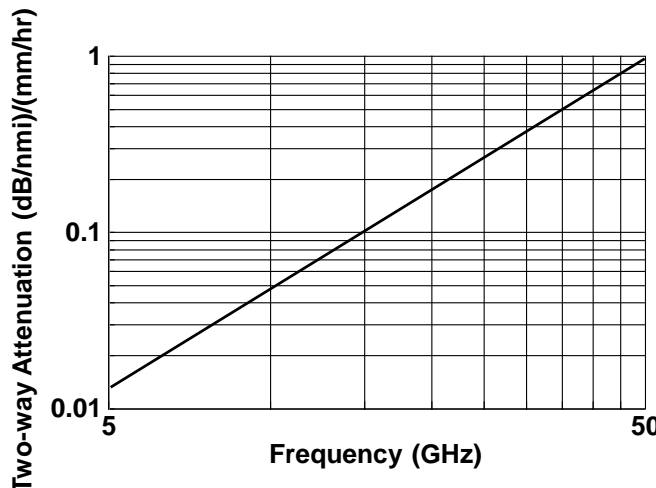
# Empirical Rain Clutter Models

- **Clear-air attenuation** ( $f$  : frequency GHz)  
 $10^{-2} f^{0.3}$  dB/km two-way
- **Attenuation in rain** ( $f$  : frequency GHz)  
 $3.7 \times 10^{-4} f^{1.85}$  (dB/km)/(mm/hr) two-way
- **Reflectivity** ( $r$  : rainfall rate mm/hr ;  $\lambda$  : wavelength, m)  
 $\eta = 6 \times 10^{-14} r^{1.6} \lambda^{-4}$  m<sup>2</sup>/m<sup>3</sup>, rain  
 $\eta = 1.2 \times 10^{-13} r^2 \lambda^{-4}$  m<sup>2</sup>/m<sup>3</sup>, snow
- **Spatial Extent** (D : diameter of rain cloud;  $r$  : mm/hr)  
 $D = 41.60 - 23.62 \log_{10}(r)$  km
- **Variation of rainfall rate with height**  
 $r/r_s = \exp(-0.2 h^2)$ , ( $r_s$  : rate at ground level;  $h$  : height, km)

Slide 29  
of 198



# Rain Attenuation



Slide 30  
of 198



## Reflectivity of Rain

Rain mm/hr	Probability in UK, %	Reflectivity, $\eta$ dBm <sup>2</sup> /m <sup>3</sup>					
		L 1.25 GHz	S 3.0 GHz	C 5.6 GHz	X 9.3 GHz	J 24 GHz	Q 35 GHz
0.25	5		-102	-91	-82	-64	-57
1	2.5	-107	-92	-81.5	-72	-54	-47
4	1	-97	-83	-72	-62	-46	-39
16	0.1		-73	-62	-53		-32

Typical values of rain reflectivity for linear polarisation

(Source, F.E.Nathanson, Radar Design Principles)

Empirical values are often used in radar design

Slide 31  
of 198



## Amplitude statistics for rain

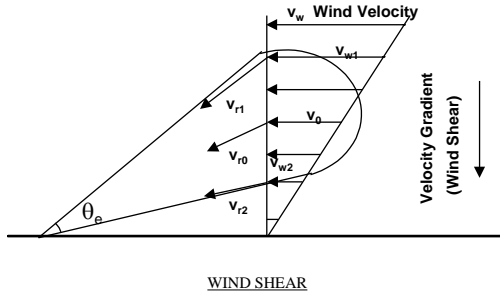
- Backscatter from rain is from multiple scatterers, distributed approximately spatially uniformly over a clutter cell.
- Local amplitude statistics should therefore be Gaussian or noise-like.
- The average intensity will vary spatially, corresponding to variations in local rainfall rate.

Slide 32  
of 198

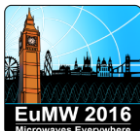


# Rain Clutter Spectrum

- Wind shear
  - Beam broadening
  - Turbulence
  - Fall velocity distribution
- $$\sigma_v^2 = \sigma_{beam}^2 + \sigma_{turb}^2 + \sigma_{fall}^2 + \sigma_{shear}^2$$



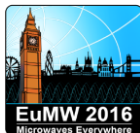
Slide 33  
of 198



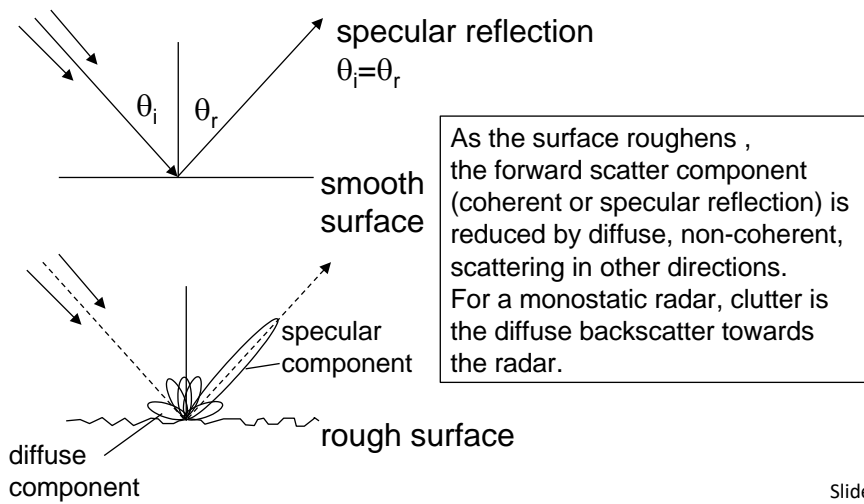
# Rain spectrum components

- WIND SHEAR
  - For a Gaussian shaped beam  $\sigma_{shear} = 0.42 kR\theta_e$ , where  $k$  is the shear gradient,  $R$  is the range from the radar and  $\theta_e$  is the antenna elevation beamwidth. A typical value of  $k$  is about  $4 \text{ ms}^{-1}\text{km}^{-1}$
- TURBULENCE
  - At altitudes up to 3 km,  $\sigma_{turb}$  can have a value of about  $1 \text{ ms}^{-1}$
- BEAM BROADENING
  - $\sigma_{beam} = 0.42 v_0 \theta_{az} \sin \theta_r$ , where  $v_0$  is the tangential wind velocity at beam centre,  $\theta_{az}$  is the antenna azimuth beamwidth, and  $\theta_r$  is the azimuth angle relative to the wind direction at beam centre. This component is usually small.
- FALL VELOCITY DISTRIBUTION
  - Finally, the distribution of vertical fall velocities amongst the raindrops will cause a spread in the velocity spectrum. A typical spread of vertical velocities is about  $1 \text{ ms}^{-1}$  so that at an elevation angle  $\phi$  we have  $\sigma_{fall} = 1.0 \sin \phi$ .

Slide 34  
of 198



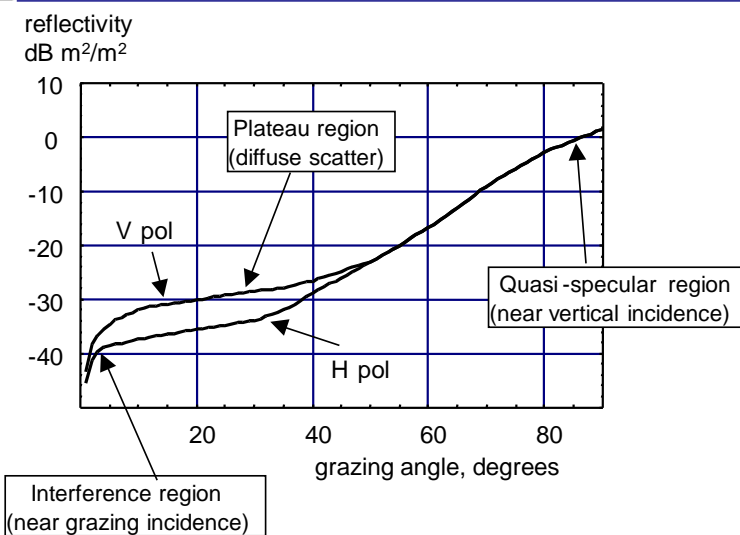
## Surface Scattering



Slide 35  
of 198



## $\sigma^0$ and grazing angle



Slide 36  
of 198



# Land Clutter

- **Key Characteristics**

Difficult to categorize.

Not spatially uniform.

Includes many large man-made and natural discrete scatterers.

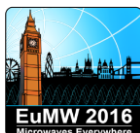
- **Distributed and discrete elements must be treated separately**

- **Often modelled by constant  $\gamma$  model for reflectivity:**

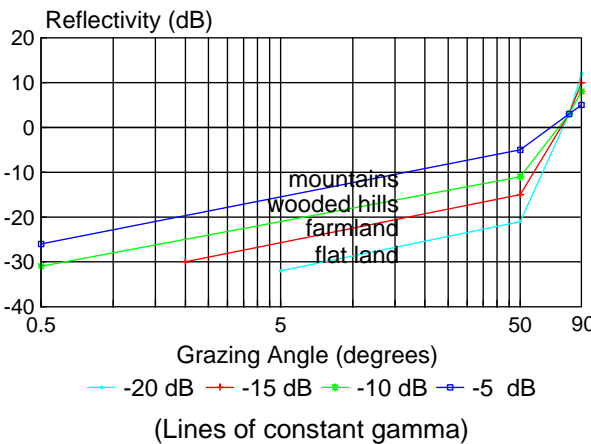
$$\sigma^0 / \sin \phi = \gamma, \text{ constant}$$

where  $\phi$  : grazing angle

Slide 37  
of 198



# Land Clutter Reflectivity



Slide 38  
of 198



## Land clutter models

- Theoretical models of clutter reflectivity rarely agree with measured results, especially at low grazing angles or for ill-defined surfaces such as land clutter.
- Empirical values are usually employed to model the variations of clutter reflectivity.
- See, for example, “Handbook of radar scattering statistics for terrain”, Artech House, 1989 .

Slide 39  
of 198



## Land clutter models

Empirical fit to data for depression angles  $\psi < 10^\circ$

$$\sigma^0 = 10 \log[A(\psi + C)^B] \exp\left[-\frac{D}{\left(1 + 0.1 \frac{\sigma_h}{\lambda}\right)}\right]$$

$\psi$  : depression angle in deg;  $\sigma_h$  : s.d. of the surface roughness in cm;  $\lambda$  : radar wavelength, cm;  $A$ ,  $B$ ,  $C$  and  $D$  are empirically derived constants.

Terrain type	<b>A</b>				<b>B</b>	<b>C</b>	<b>D</b>
Frequency (GHz)	15	9.5	5	3	All	All	All
Soil, sand and rocks	0.05	0.025	0.0096	0.0045	0.83	0.0013	2.3
Grass and crops	0.079	0.039	0.015	0.0071	1.5	0.012	0.0
Trees	0.019	0.003	0.0012	0.00054	0.64	0.002	0.0
Urban	2.0	2.0	0.779	0.362	1.8	0.015	0.0

[Currie N.C., Clutter Characteristics and Effects, in *Principles of Modern Radar*, J.L. Eaves and E.K. Ready, Eds., New York, Van Nostrand Reinhold, 1987, pp 281 -340 ]

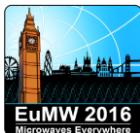
Slide 40  
of 198



# Land clutter amplitude statistics

- Most ground clutter is a mixture of discrete and distributed scatterers.
- Areas of uniform terrain, such as farmland or forest, may be amenable to modelling as distributed clutter, especially at higher grazing angles.
- At low grazing angles ground clutter may become very patchy (due to shadowing) and very spiky.
- Early work used the lognormal PDF, to account for the long tailed distributions observed (often due to inclusion of large discrete scatterers).
- Weibull and K distribution models have also been used to fit to observed data [J.B. Billingsley, *Low-angle radar land clutter – Measurements and empirical models*, William Andrew Publishing, Norwich, NY, 2002].
- These PDF models are discussed further in section on sea clutter.

Slide 41  
of 198



# Discrete scatterers on land

- Land clutter will often contain many discrete scatterers, some very large.
- Barton\* analysed a number of results to propose:
  - $10^4 \text{ m}^2$  scatterers with a density of  $0.2/\text{km}^2$
  - $10^3 \text{ m}^2$  scatterers with a density of  $0.5/\text{km}^2$
  - $10^2 \text{ m}^2$  scatterers with a density of  $2.0/\text{km}^2$
- Long\*\* has proposed:
  - $10^6 \text{ m}^2$  scatterers with a density of  $0.004/\text{km}^2$
  - $10^5 \text{ m}^2$  scatterers with a density of  $0.04/\text{km}^2$

\* Barton D.K., *Radar System Analysis and Modeling*, Artech House, 2005

\*\* Long W.H.D., Mooney D. and Skillman W.A., Pulse Doppler Radar, in *Radar Handbook*, 2<sup>nd</sup> Edition, M. Skolnik (Ed.), New York, McGraw Hill, 1990, chap. 17, pp. 17.11-17.16

Slide 42  
of 198



## Billingsley spectrum model

$$P_{tot}(v) = \frac{r}{r+1} \delta(v) + \frac{1}{r+1} P_{ac}(v)$$

$$P_{ac}(v) = \frac{\beta}{2} \exp(-\beta|v|) , \quad -\infty < v < \infty$$

$$10\log_{10} r = -15.5\log_{10} w - 12.1\log_{10} f_0 + 63.2$$

$P_{tot}(v)$  : the power spectral density from a cell containing windblown clutter

$\delta(v)$  : delta function

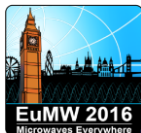
$v$  : Doppler velocity in m/s

$w$  : wind speed in miles per hour

$f_0$  : radar carrier frequency in MHz

J.B.Billingsley, Exponential decay in windblown radar ground clutter Doppler spectra: multifrequency measurements and model, MIT Lincoln Laboratory, Technical Report 997, 29 July 1996

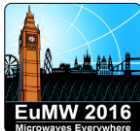
Slide 43  
of 198



## Billingsley spectrum model

Wind conditions	Wind Speed (mph)	Exponential ac shape parameter $\beta$ $(\text{m/s})^{-1}$	
		Typical	Worst case
Light air	1-7	12	-
Breezy	7-15	8	-
Windy	15-30	5.7	5.2
Gale Force (est)	30-50	4.3	3.8

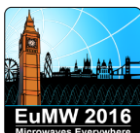
Slide 44  
of 198



## Sea Clutter

- Reflectivity of sea clutter dependent on:
  - Wind speed (sea state)
  - Wind direction
  - Radar frequency
  - Grazing angle
  - Polarisation
- Sea state dependent on fetch and duration and is not a reliable indicator of reflectivity.
- Many good empirical models for reflectivity  
Nathanson, Georgia Institute of Technology etc.

Slide 45  
of 198



## Empirical Models of $\sigma^0$ for Sea

- **Nathanson**

Tabulated values as function of sea state, given in  
“Radar Design Principles”

Does not show variation with wind direction

- **Georgia Institute of Technology**

Contains representation of interference effects,  
wind speed and direction, wave height and  
polarisation, adjusted empirically to fit  
observed data.

Slide 46  
of 198



## GIT Model, 1 - 10 GHz

Reflectivity equations

$$\sigma_0(H) = 10 \log_{10} [3.9 \times 10^{-6} \lambda \psi^{0.4} G_a G_u G_w]$$

$$\sigma_0(V) = \begin{cases} \sigma_0(H) - 1.05 \ln(h_a + 0.015) + 1.09 \ln(\lambda) + 1.27 \ln(\psi + .0001) + 9.70 & \text{(3 to 10 GHz)} \\ \sigma_0(H) - 1.73 \ln(h_a + 0.015) + 3.76 \ln(\lambda) + 2.46 \ln(\psi + .0001) + 22.2 & \text{(below 3 GHz)} \end{cases}$$

where  $\sigma_0(H)$  and  $\sigma_0(V)$  are the reflectivities for V and H polarisations.

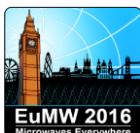
The adjustment factors are

$$G_a = \frac{a^4}{1+a^4}; \quad G_u = \exp[0.2 \cos \phi (1-2.8\psi) (\lambda+0.015)^{-0.4}] \quad G_w = \left[ \frac{1.94 V_w}{(1+V_w/15.4)} \right]^q$$

with  $q = 1.1/(\lambda + 0.015)^{0.4}$  and  $a = (14.4\lambda + 5.5)\psi h_a/\lambda$

M.M. Horst, F.B. Dyer, M.T. Tuley, Radar Sea Clutter Model, IEEE International Conf. Antennas and Propagation, November 1978, pp 6 - 10

Slide 47  
of 198



## GIT Model, 10 - 100 GHz

Reflectivity equations

$$\sigma_0(H) = 10 \log[5.78 \times 10^{-6} \psi^{0.547} G_a G_u G_w]$$

$$\sigma_0(V) = \sigma_0(H) - 1.38 \ln(h_a) + 3.43 \ln(\lambda) + 1.31 \ln(\psi) + 18.55$$

where  $\sigma_0(H)$  and  $\sigma_0(V)$  are the reflectivities for V and H polarisations.

The adjustment factors are

$$G_a = \frac{a^4}{1+a^4}; \quad G_u = \exp[0.25 \cos \phi (1-2.8\psi) \lambda^{-0.33}]$$

$$G_w = \left[ \frac{1.94 V_w}{(1+V_w/15.4)} \right]^q$$

with  $q = 1.93 \lambda^{-0.04}$  and  $a = (14.4 \lambda + 5.5)\psi h_a/\lambda$

There are some discontinuities between the 1 – 10 GHz and 10 – 100 GHz models, so care should be taken if using both models to predict performance

Slide 48  
of 198



# GIT Clutter Models

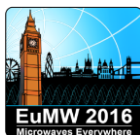
Units and symbols:

$\sigma_0(H)$ , $\sigma_0(V)$	:	reflectivity for H and V polarisations, dB m <sup>-2</sup> /m <sup>2</sup>
$h_a$	:	average wave height, m ( $h_a \approx 4.52 \cdot 10^{-3} V_w^{2.5}$ )
$\lambda$	:	radar wavelength, m
$V_w$	:	wind velocity, m/s
$\psi$	:	grazing angle, rad ( $0.1 \leq \psi \leq 10$ degrees)
$\phi$	:	look direction relative to wind direction, rad

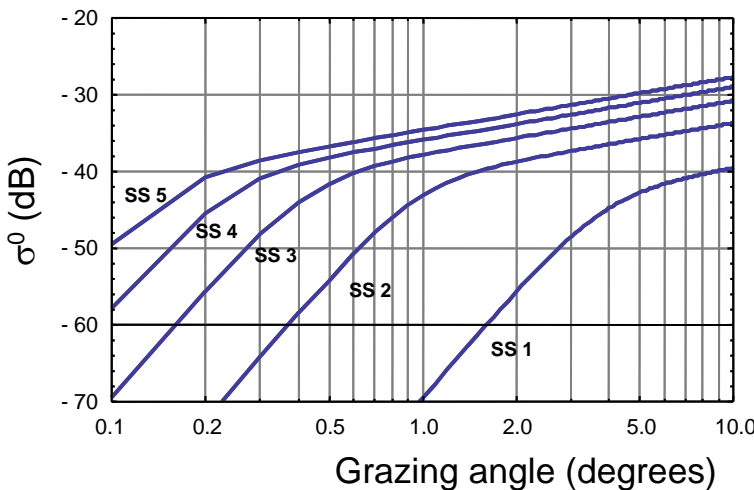
The windspeed can be written in terms of sea state as

$$V_w = 3.16 s^{0.8}$$

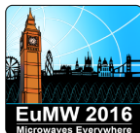
Slide 49  
of 198



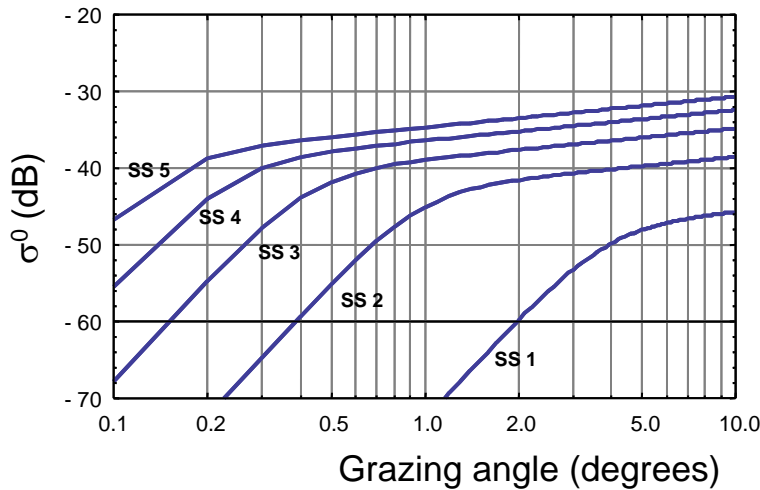
# GIT Model, VV Pol



Slide 50  
of 198



## GIT Model, HH Pol



Slide 51  
of 198



## Douglas Sea State

Sea state is described in terms of significant wave height,  $h_{1/3}$ , the mean of the peak-to-trough height of highest 1/3 of waves

Douglas Sea State	Description	Wave height $h_{1/3}$ ft	Wind speed kts	Fetch nmi	Duration hr
1	Smooth	0-1	0-6		
2	Slight	1-3	6-12	50	5
3	Moderate	3-5	12-15	120	20
4	Rough	5-8	15-20	150	23
5	Very Rough	8-12	20-25	200	25
6	High	12-20	25-30	300	27
7	Very high	20-40	30-50	500	30
8	Precipitous	>40	>50	700	35

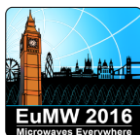
Slide 52  
of 198



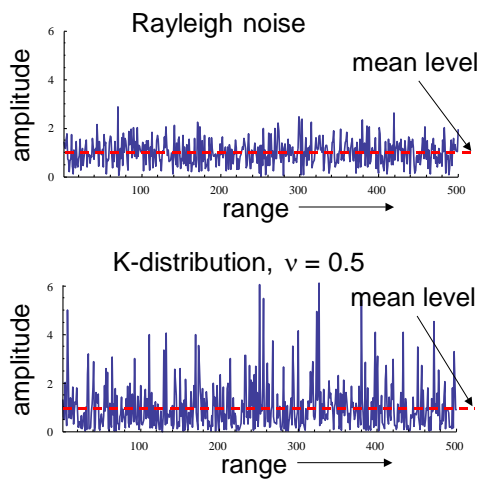
## Sea Clutter Amplitude Stats

- **Large grazing angles and long pulse lengths:**  
Gaussian statistics  
Rayleigh envelope
- **Small grazing angles, short pulse lengths:**  
“Spiky” clutter  
Long-tailed distributions
- **Spiky clutter distribution shape dependent on:**  
Grazing angle  
Spatial resolution  
Polarisation  
Swell magnitude and direction

Slide 53  
of 198



## Non-Gaussian Statistics

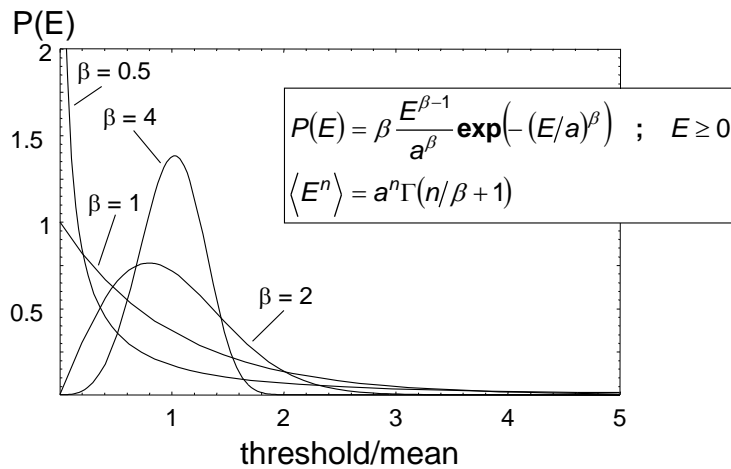


- Rayleigh noise and K-distributed clutter ( $v=0.5$ ) with mean value 1.
- K-distribution illustrates “spiky” clutter having a “long tailed” amplitude distribution.
- Rayleigh noise derives from standard Gaussian statistics.

Slide 54  
of 198



## Weibull Distribution



55

Slide 55  
of 198

## Log-Normal Distribution

Variate expressed in dB has a Gaussian distribution

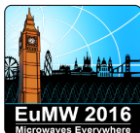
$$P(z) = \frac{1}{z\sqrt{2\pi\sigma^2}} \exp\left(-\frac{(\log[z] - m)^2}{2\sigma^2}\right); z \geq 0$$

$m$  : median of  $\log[z]$

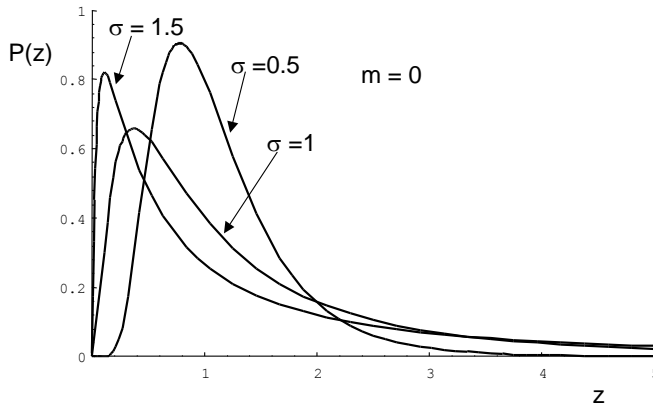
$\sigma$  : standard deviation of  $\log[z]$

$$\langle z^n \rangle = \exp\left(nm + n^2\sigma^2/2\right)$$

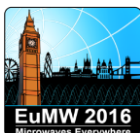
Slide 56  
of 198



## Log-Normal PDF

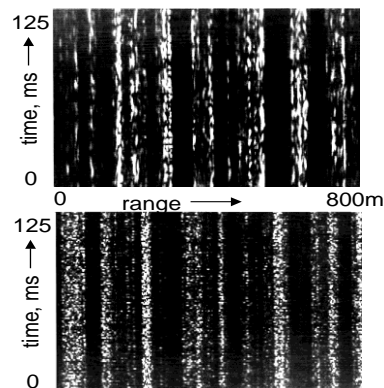


Slide 57  
of 198



## Sea Clutter

- The figures show recordings of sea clutter as a range-time intensity plot, with 125 successive returns at a PRI of 1ms from a range patch of 800m.
- The upper figure shows fixed frequency returns. At a given range the returns exhibit a correlation time of  $\sim 10$ ms.
- The lower figure shows frequency agile returns. Now returns at each range are decorrelated from pulse to pulse but the swell pattern is not affected.



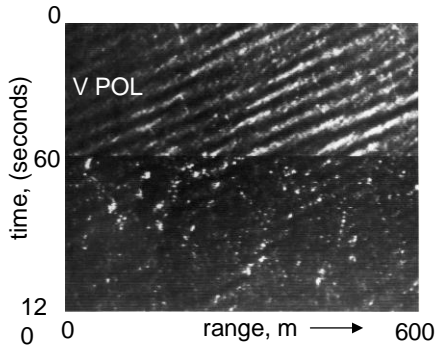
K.D.Ward, R.J.A.Tough and S.Watts, "Sea Clutter: Scattering, the K Distribution and Radar Performance", 2<sup>nd</sup> Edition, Institution of Engineering and Technology, 2013

Slide 58  
of 198



## Sea Clutter

- The fluctuating component (speckle) has here been removed by adding successive pulses. After 60sec the polarisation changes from VV to HH. The V POL returns show a clear swell-like component whilst the H POL returns show short lived (~1 s) clutter "spikes" which still appear to be associated with the swell peaks.
- Radar: I-band, grazing angle 1.5 deg, range 5 km, pulse length 28 ns.



Slide 59  
of 198



## Compound K-Distribution (1)

The backscatter from any clutter cell is assumed to be from multiple scatterers with a Rayleigh amplitude distribution

$$P(E | x) = \frac{2E}{x} \exp(-E^2/x)$$

where  $\overline{E^2} = x$

The mean intensity,  $x$ , may vary spatially and it has been found that it can be modelled by a Gamma distribution:

$$P_c(x) = \frac{b^\nu}{\Gamma(\nu)} x^{\nu-1} \exp(-bx) ; 0 \leq x \leq \infty$$

Slide 60  
of 198



## Compound K-Distribution (2)

The overall distribution of the clutter envelope is now given by:

$$P(E) = \int_0^{\infty} P_c(x) P(E | x) dx = \frac{4b^{(\nu+1)/2}}{\Gamma(\nu)} E^\nu K_{\nu-1}(2E\sqrt{b})$$

where  $b$  is a scale parameter

$K_\nu(E)$  is a modified Bessel function,  
and  $\nu$  is a shape parameter.

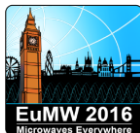
The nth moments of  $x$  are :

$$\langle x^n \rangle = \frac{1}{b^n} \frac{\Gamma(\nu+n)}{\Gamma(\nu)}$$

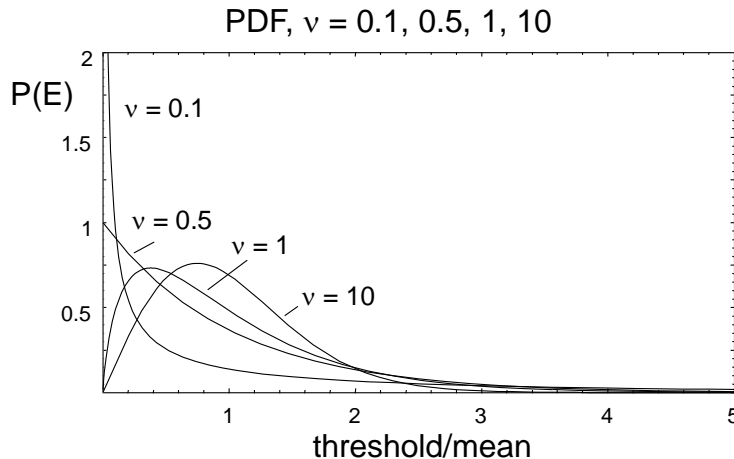
The nth moments of the K distribution,  $E$ , are :

$$\langle E^n \rangle = b^{-n/2} \frac{\Gamma(1+n/2)\Gamma(\nu+n/2)}{\Gamma(\nu)}$$

Slide 61  
of 198



## K-Distribution



Slide 62  
of 198



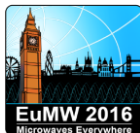
# K-Distribution Shape Parameter

- Empirical formulae have been developed for this distribution in sea clutter. For X-band:

$$\log(v) = (2/3)\log(\phi) + (5/8)\log(L \rho/4.2) + \sigma - k$$

$\phi$	:	grazing angle, degrees ( $0.1^\circ < \phi < 10^\circ$ )
$L$	:	across-range resolution, m ( $100 < L < 950$ )
$\rho$	:	range resolution (m)
$\sigma$	=	-1/3 , up-swell or down-swell
	=	+1/3 , across-swell
	=	0 , no-swell or intermediate directions
$k$	=	1 for Vertical polarisation
	=	1.7 for Horizontal polarisation

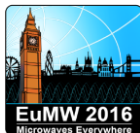
Slide 63  
of 198



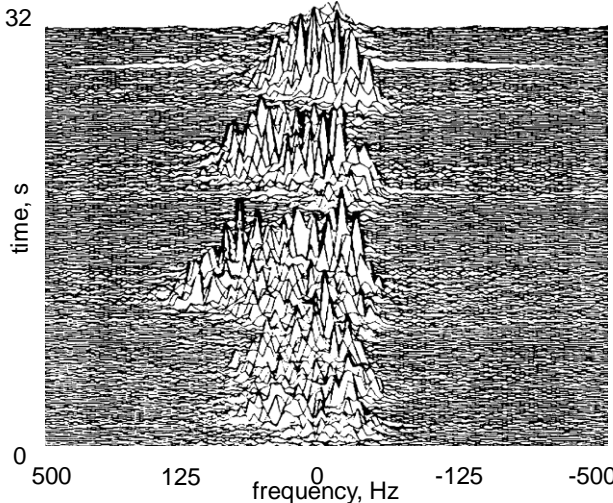
# Coherent Clutter

- The coherent return from K-distributed clutter can be represented as a Gaussian variate modulated by an underlying Gamma distributed power.
- This is a representation of a Spherically Invariant Random Vector (SIRV).
- This approach still has some limitations to sea clutter where there is a relationship between spectral shape and local intensity and the envelope of the returns varies as a function of Doppler across the spectrum.

Slide 64  
of 198

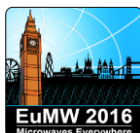


## Spectrum of Sea Clutter



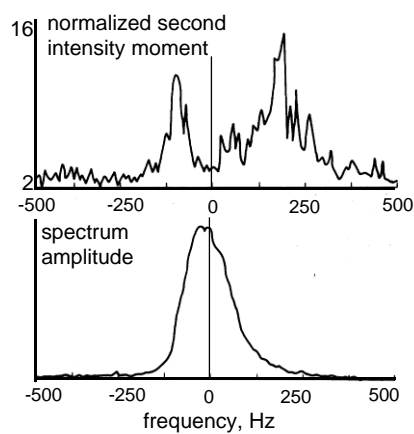
Time history  
of sea clutter  
Doppler  
spectra from  
a single  
range cell  
(Sea state 2)

Slide 65  
of 198



## Average spectrum

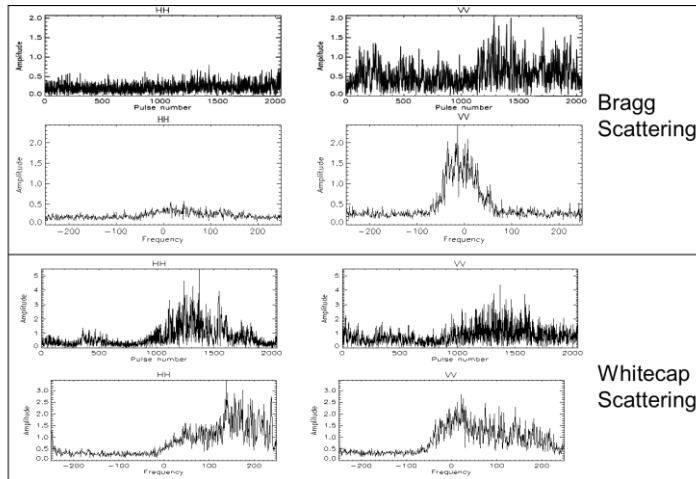
- V POL sea clutter spectrum averaged over many time periods, with the normalized second intensity moment  $\langle z^2 \rangle / \langle z \rangle^2$  showing increased non-Gaussian ("spiky") characteristics in edges of the spectrum.
- Average spectrum is asymmetric and with non-zero mean associated with wind direction. Doppler offset is sinusoidal with wind direction, zero looking across-wind and with larger offset for H pol than V pol



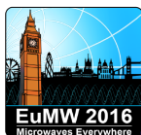
Slide 66  
of 198



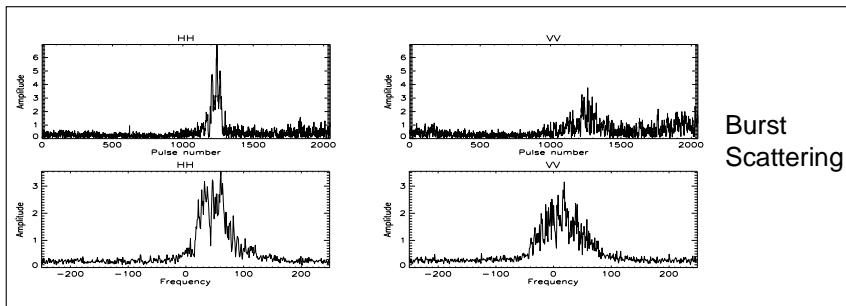
# Doppler signatures



Slide 67  
of 198



# Doppler signatures



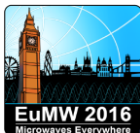
Slide 68  
of 198



# Modelling Sea Clutter Spectra

- Some useful empirical results are given here.
- Simple low grazing angle model, for mean velocity of Doppler spectrum  $V_{VV}$  and  $V_{HH}$  and half-power width  $\Delta$ , looking upwind or downwind, with wind speed  $U$  ( $ms^{-1}$ ):
  - $V_{VV} = 0.25 + 0.18 U$  ( $ms^{-1}$ )
  - $V_{HH} = 0.25 + 0.25 U$  ( $ms^{-1}$ )
  - $\Delta = 0.24 U$  ( $ms^{-1}$ )
  - Mean velocity will be zero looking crosswind, with a co-sinusoidal variation over look direction.
- The variation of Doppler spectra with grazing angle,  $\theta$ , at higher grazing angles can be modelled as:
  - $V_{VV}$  and  $V_{HH} \propto \cos(\theta)$
  - For  $\theta > 50^\circ$ ,  $V_{VV} \approx V_{HH}$ , with similar spectrum shapes

Slide 69  
of 198



# Modelling Sea Clutter Spectra

- Model based on observations of sea clutter at low and medium grazing angles
- Spectrum mean Doppler shift is correlated with local intensity (i.e. process is not SIRV)
- Spectrum width fluctuates randomly
- Combined with compound distribution (e.g. K distribution) model can describe time-varying and range-varying spectra

K.D.Ward, R.J.A.Tough and S.Watts, "Sea Clutter: Scattering, the K Distribution and Radar Performance", 2<sup>nd</sup> Edition, Institution of Engineering and Technology, 2013.  
 Watts, S., Rosenberg, L., Bocquet, S. and Ritchie, M., Doppler spectra of medium grazing angle sea clutter; part 1: characterisation, IET Radar Sonar Navig., Vol. 10, Iss. 1, Jan 2016, pp. 24 – 31.  
 Watts, S., Rosenberg, L., Bocquet, S. and Ritchie, M., Doppler spectra of medium grazing angle sea clutter; part 2: exploiting the models, IET Radar Sonar Navig., Vol. 10, Iss. 1, Jan 2016, pp. 32 – 42.

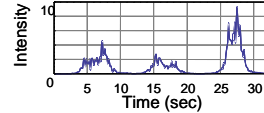
Slide 70  
of 198



# Modelling Sea Clutter Spectra

Gamma PDF, correlated over time, of mean intensity

$$p_c(x) = \frac{b^\nu}{\Gamma(\nu)} x^{\nu-1} \exp(-bx) ; \quad 0 \leq x \leq \infty$$

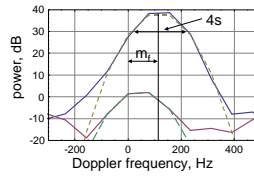


Gaussian-shaped PSD

$$G(f, x, s) = \frac{x}{\sqrt{2\pi} s} \exp\left[-\frac{(f - m_f(x))^2}{2s^2}\right]$$

$m_f(x)$  : mean Doppler frequency

$s$  : spectrum width (standard deviation of Gaussian spectrum).

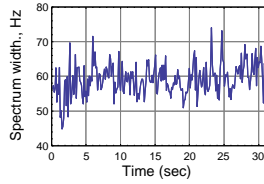


Normal PDF for spectrum width,  $s$ :

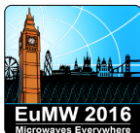
$$p_s(s) = \frac{1}{\sqrt{2\pi} \sigma_s} \exp\left[-\frac{(s - m_s)^2}{2\sigma_s^2}\right] ; \quad 0 \leq s \leq \infty$$

where  $m_s$  : mean spectrum width

$\sigma_s^2$  : variance of spectrum width.



Slide 71  
of 198



## Clutter modelling conclusions

- Models of clutter are used to predict performance, compare performance of different systems and to help develop improved detection processors
- Models may be based on theoretical approximations to the environment or, more usually, on empirical measurements.
- Models usually represent typical or average conditions.
- The real environment may vary considerably from the model, even for apparently identical conditions.
- Practical radar processors must be robust to “deviations” from the models.

Slide 72  
of 198



## Uses of clutter models

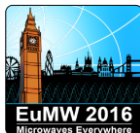
Slide 73  
of 198



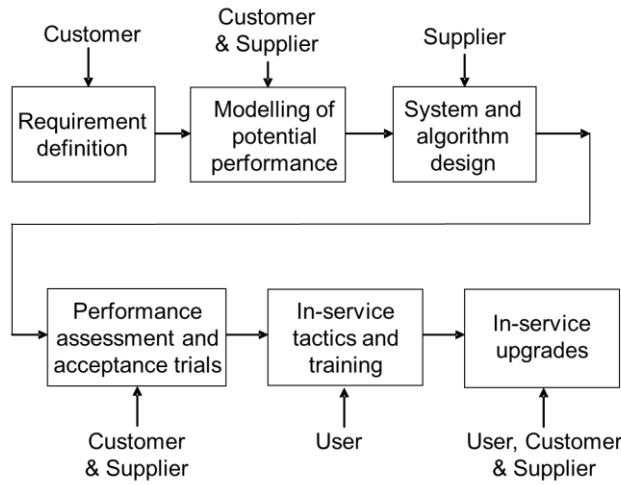
## Uses of clutter models

- Clutter models are used in various ways at each stage of the life-cycle of a radar
- Requirements definition and specification
  - What the customer wants
- Modelling of predicted performance
  - Possibly as part of a procurement competition
- Design of radar waveforms and signal/data processing
- Demonstration of performance and acceptance into service by a customer and/or user.
- Training of personnel
- In-service upgrades of equipment
  - New user requirements
  - Technology upgrades

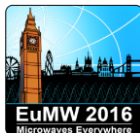
Slide 74  
of 198



# The radar life cycle



Slide 75  
of 198



## Uses of clutter models

### Radar Specifications

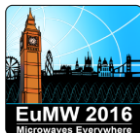
Slide 76  
of 198



## Modelling and specifications

- Modelling forms an essential part of the specification process for a complex radar
  - derivation of performance specification
  - link between basic performance measures and operational performance

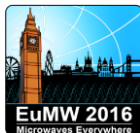
Slide 77  
of 198



## Environment specification

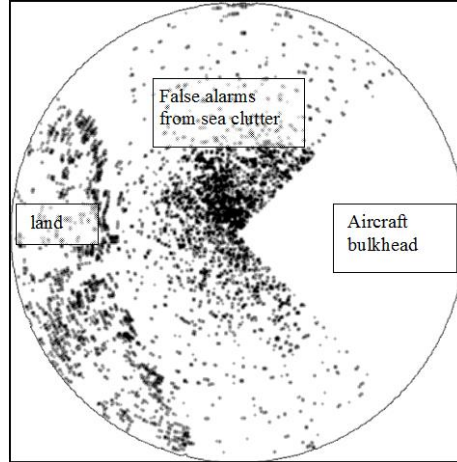
- Typical requirement might be stated as:  
*Detect a stationary target on the sea surface with an RCS of 1 m<sup>2</sup> in SS4 at 20 nmi range, with P<sub>d</sub> = 0.9 and 1 false alarm a minute.*
- None of these requirement points is capable of being accurately measured without further qualification.
- Specify performance in terms of models, such as:
  - RCS
    - Swerling models
  - Sea State
    - Reflectivity models
    - Amplitude statistics models
    - Spatial correlation models

Slide 78  
of 198



## Specification – false alarms

- False alarm map
- Specification should acknowledge the possibility of spatial variations of alarm density, areas of low sensitivity etc.
- Low false alarm rates are very difficult to measure

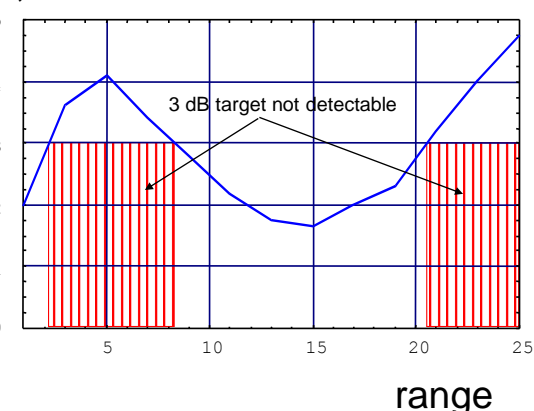


Slide 79  
of 198



## Detection range

- Minimum detectable rcs, dB
- RCS v. range, in clutter
- What is the detection range for a 3 dB target?
- Intermediate-range detection limited by clutter
- Long-range detection limited by noise.



Slide 80  
of 198



## Uses of clutter models

### Performance Prediction

Slide 81  
of 198



## Performance prediction

- Detection in clutter is initially predicted using the radar range equation, with:
  - Clutter characteristics (as a function of sea conditions, viewing geometry and radar parameters)
    - Normalised radar cross-section,  $\sigma^0$
    - Doppler spectrum
    - Amplitude statistics
    - Spatial correlation
    - Effects of pulse-to-pulse frequency agility
  - Detection processing
    - Effects of Doppler filtering
    - Effects of non-coherent integration (pulse-to-pulse and scan-to-scan), including the effects of frequency agility, antenna scan rate, integration algorithms etc.
  - Signal processing “losses” - performance relative to some idealised baseline (e.g. CFAR loss, cusping losses, quantisation loss etc.).

Slide 82  
of 198



## Uses of clutter models

### Radar Design

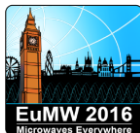
Slide 83  
of 198



## Radar design and clutter

- Many signal and data processing techniques require a good understanding of clutter for their design:
  - AGC
  - Pulse-to-pulse non-coherent integration.
  - Coherent processing (e.g. pulse Doppler processing)
  - CFAR design
  - Trackers
  - etc.

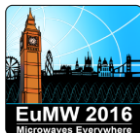
Slide 84  
of 198



# Engineering development

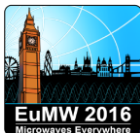
- During development, design is continually assessed in terms of impact on performance, often analysed in terms of processing “losses”
- Typical examples of signal processing losses are
  - beamshape loss of pulse-to-pulse integration (compared to ideal filter)
  - pulse compression loss (compared to the ideal matched filter)
  - quantisation losses
  - range cusping loss
  - CFAR loss
- Many of these losses are different for targets and clutter and may depend on the prevailing conditions
- Good clutter models help to inform design decisions

Slide 85  
of 198



## Measurement of Radar Performance

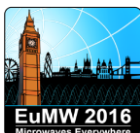
Slide 86  
of 198



# Measurement of Performance

- Factory measurements
  - Noise-limited performance can be estimated accurately from factory measurements of components and sub-assemblies.
- Trials
  - An essential part of most customer acceptance processes but many radar performance features either cannot be measured in a trial alone due to:
    - Cost of long trials campaigns
    - Unknown real target and clutter characteristics compared with specified characteristics.
    - Measurement and observation uncertainties in dynamically changing scenarios
- Modelling and Simulation
  - May be the only way of measuring some radar performance features
  - May be needed to interpret trial results

Slide 87  
of 198



# Modelling and Simulation

- Performance usually predicted by modelling, which must be agreed between customer and supplier
- Models often based on extensive trials ( $\sigma^\circ$  etc.)
- Analytic models do not predict or quantify adaptive performance
- Simulation may be used to quantify adaptive performance using synthetic scenarios
- Use trials to validate (prove) modelling method and adaptive behaviour but not the whole model
- Combine with instrumented trials to extrapolate observations

Slide 88  
of 198



## Other uses of clutter models

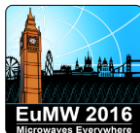
Slide 89  
of 198



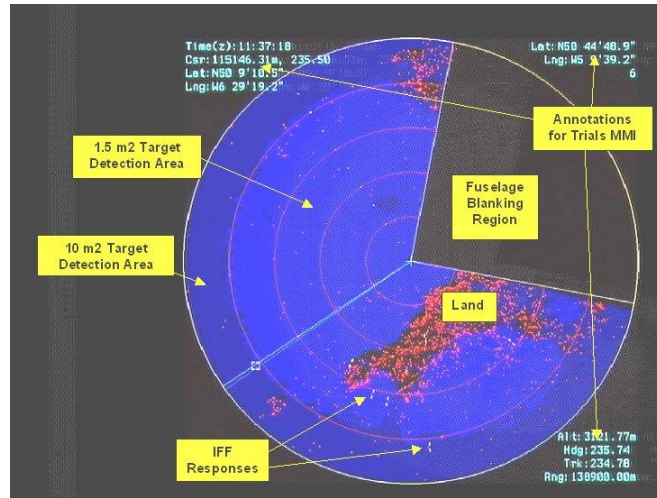
## Other uses of clutter models

- Operator aids
  - Probability of detection display
- Operator training
  - Synthetic radar returns as input to real-time radar simulator
- Through-life maintenance and improvement
  - Continuous radar performance monitoring compared with modelling predictions
  - Identify shortcoming and propose improvements

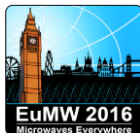
Slide 90  
of 198



# Probability of Detection Display



Slide 91  
of 198



**EURAD**  
**2016**

The 13th European Radar Conference

## Simulation of Sea Clutter

Keith D Ward

Igence Radar Ltd, UK

keith.ward@igence.com

Slide 92  
of 198



# Introduction

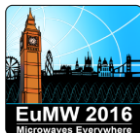
Radar clutter simulation can be done at a number of different levels

- Electromagnetic simulation
- Statistical simulation
- Simulation of the output of radar processing

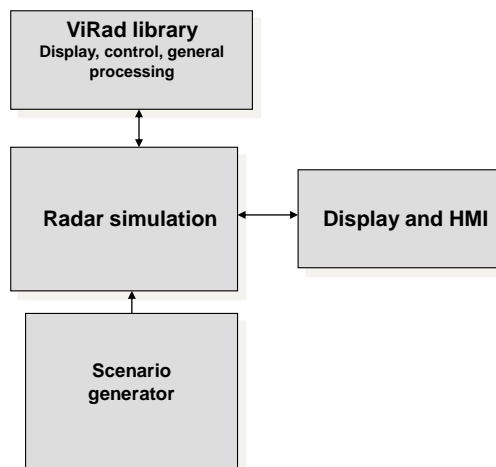
The results can be used to simulate and emulate entire radar systems for use throughout their lifecycle

It is important to model the environment and scenario accurately, and to incorporate the effects of these in the sea clutter simulation

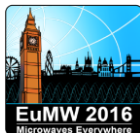
Slide 93  
of 198



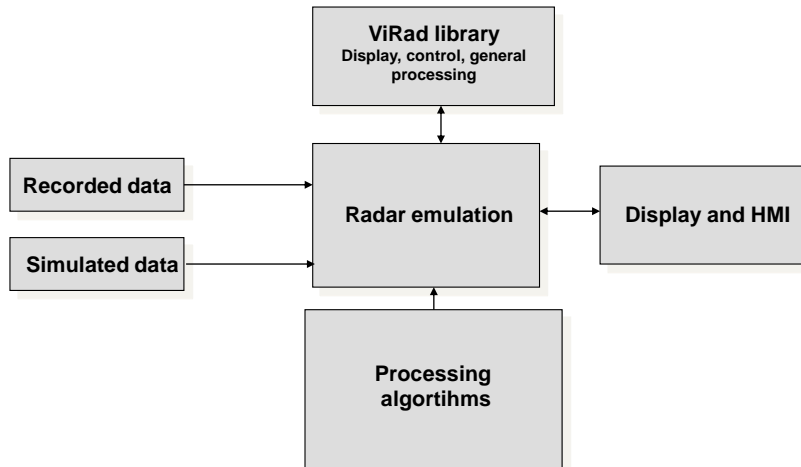
# Radar system simulation



Slide 94  
of 198



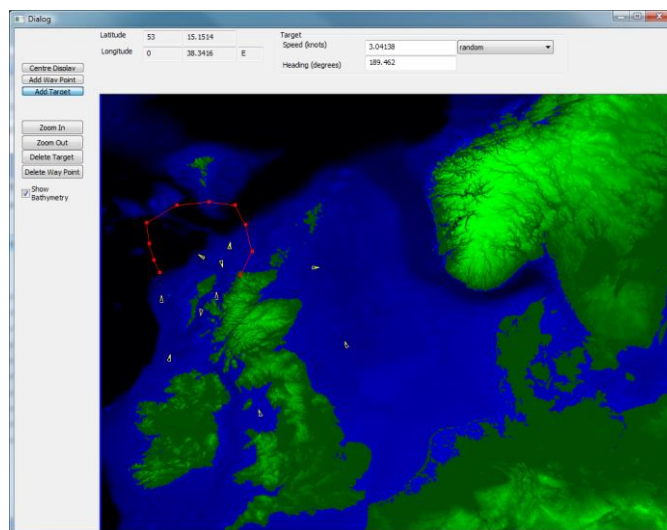
## Radar system emulation



Slide 95  
of 198



## Scenario generation



Slide 96  
of 198



## Statistical simulation

Slide 97  
of 198



## Statistical simulation

A stationary Gaussian process is fully defined by its power spectrum or autocorrelation function (ACF) and can be simulated using FFTs

Non-Gaussian processes can be generated from nonlinear transformation (MNLT) of a Gaussian process. It is possible to reproduce the required ACF, but the higher correlation properties are ‘built-in’ to the MNLT

For sea clutter it is best to use the compound K distribution and to simulate the Gamma component using MNLT

Slide 98  
of 198



# Statistical simulation

## Correlated Gamma process using MNLT

Cumulative distribution of Gaussian and required (Gamma)

$$\int_{\eta}^{\infty} P_{\text{dist}}(\eta') d\eta' = \frac{1}{\sqrt{2\pi}} \int_{x}^{\infty} \exp(-x^2/2) dx = \frac{1}{2} \operatorname{erfc}(x/\sqrt{2})$$

$$\int_{Q_{\text{dist}}(\zeta)}^{\infty} P_{\text{dist}}(\eta) d\eta = \zeta$$

Match to give Gamma variate from Gaussian variate

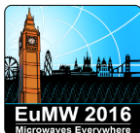
$$\eta(x) = Q_{\text{dist}}(\operatorname{erfc}(x/\sqrt{2})/2)$$

ACF of Gamma in terms of ACF of Gaussian

$$\langle \eta(0)\eta(t) \rangle = \frac{1}{\pi} \sum_{n=0}^{\infty} \frac{R_G(t)^n}{2^n n!} \left( \int_{-\infty}^{\infty} dx \exp(-x^2) H_n(x) Q_{\text{dist}}(\operatorname{erfc}(x)/2) \right)^2$$

Solve to give  $R_G(t)$  in terms of  $\langle \eta(0)\eta(t) \rangle$

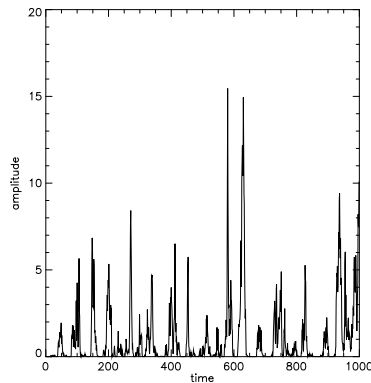
Slide 99  
of 198



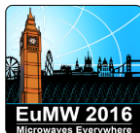
# Statistical simulation

An amplitude time series of a Gamma process with  $\nu=0.3$  and a correlation function given by equation

$$\langle \eta(0)\eta(t) \rangle = 1 + \frac{\exp(-t/10)\cos(t/8)}{\nu}$$



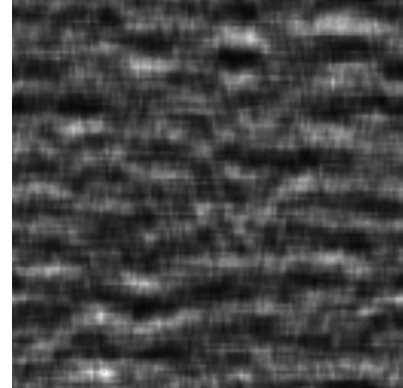
Slide 100  
of 198



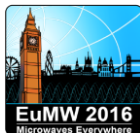
## Statistical simulation

A Gamma distributed random field with  $\nu=5$  and a correlation function given in equation

$$\langle \eta(0,0)\eta(x,y) \rangle = 1 + \frac{\exp\left(-\frac{x+y}{10}\right) \cos\left(\frac{\pi y}{8}\right)}{\nu}$$



Slide 101  
of 198

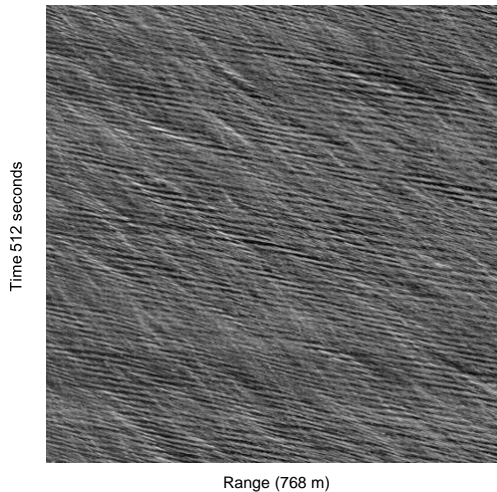


## Spatial and temporal correlations

Slide 102  
of 198



## Spatial and temporal



Range time intensity  
plot of sea clutter data

(stationary antenna,  
sea state 4)

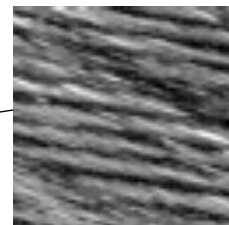
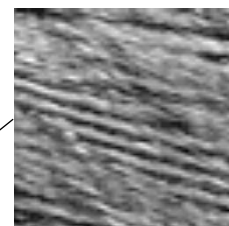
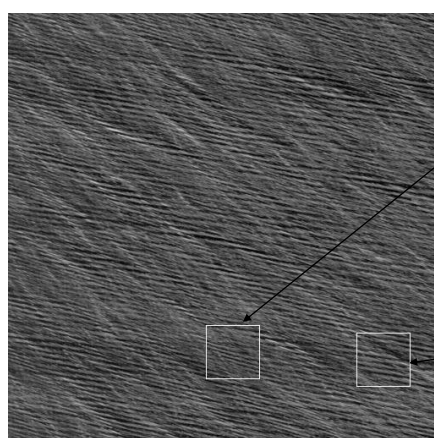
Slide 103  
of 198



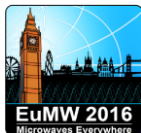
## Spatial and temporal

Different regions are dominated by different frequencies  
Therefore the data looks non-stationary

Time 512 seconds

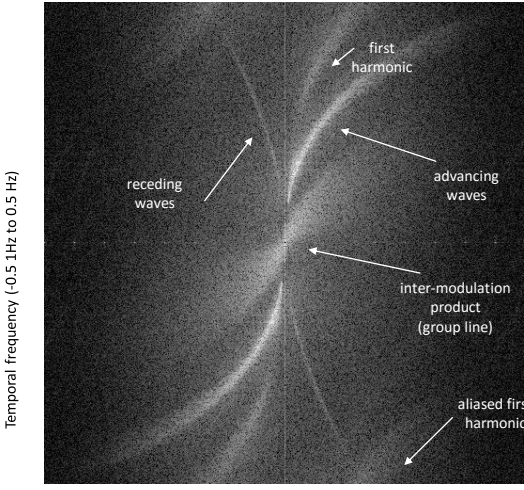


Slide 104  
of 198



## Spatial and temporal

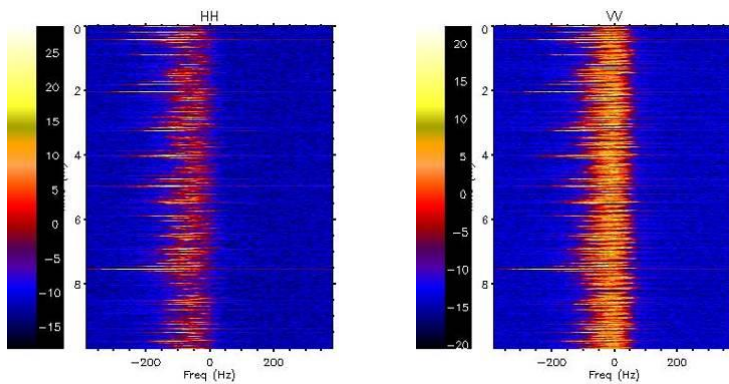
2D Fourier transform of  
Range-Time plot  
(log intensity)



Slide 105  
of 198



## Spatial and temporal



Doppler-Time-intensity plots

Slide 106  
of 198



## Open ocean modelling

Slide 107  
of 198



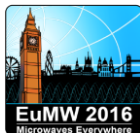
## Open ocean

### EM scattering

- Physical optics at high angles
- Composite model at intermediate angles
- Composite model (with shadowing and multipath) and breaking wave contribution at low grazing angles

All models have been reasonably well validated for NRCS in the open sea

Slide 108  
of 198

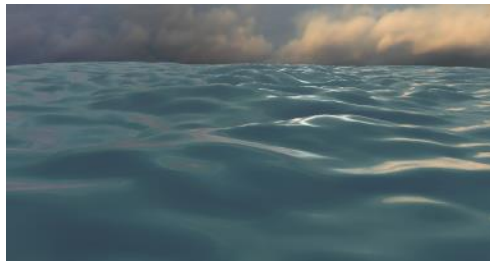


# Open ocean

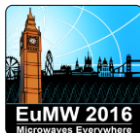
## Open ocean modelling

Linear addition of sinusoids

- Random amplitudes and phases
- Weighted with average power spectrum
- Result is Gaussian distributed surface
- Nonlinear effects and breaking waves are introduced using a ‘breaking criterion’ of the vertical acceleration downwards being greater than  $g/2$

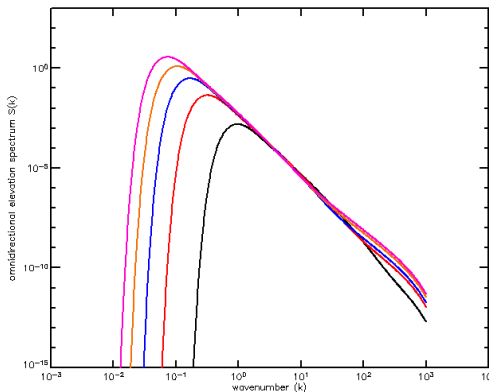


Slide 109  
of 198



# Open ocean

## Elfouhaily omnidirectional wave spectrum

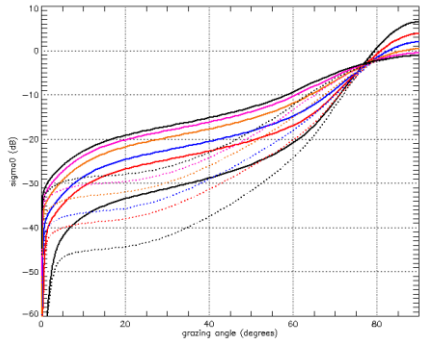
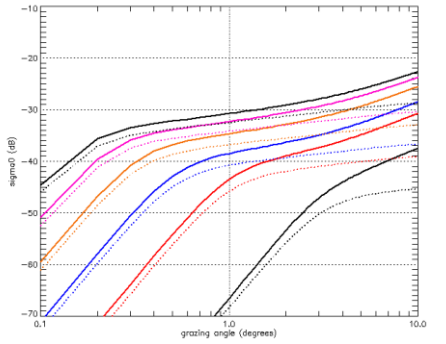


Slide 110  
of 198



# Open ocean

Open sea NRCS at all grazing angles  
(VV and HH, sea states 1 to 6)



Slide 111  
of 198



## Sea Clutter in Littoral environments

Slide 112  
of 198



# Littoral environments

## Introduction

- Many radar systems are used in littoral environments
- They have been found experimentally to have inferior performance due to the characteristics of littoral sea clutter and propagation
- The differences between open ocean and littoral sea clutter are not well modelled – every littoral environment is different
- Therefore the design, optimisation, testing, and operation of these radars in the littoral environment is, at best, *ad hoc*

Slide 113  
of 198



# Littoral environments

## Littoral water wave dynamics

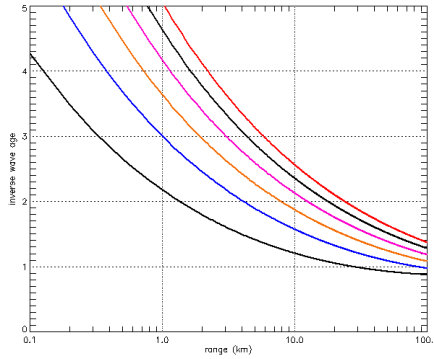
- Four effects introduced for littoral environment
  - Change of wave spectrum due to limited fetch
  - Change of wave spectrum due to local current variation
  - Wave refraction due to depth changes
  - Increased breaking due to shallow water
- All of these processes should really be modelled together
- Very difficult to do over wide area
- We model sequentially using approximations (many derived for CGI)

Slide 114  
of 198



# Littoral environments

## Littoral waters effect: (1) limited fetch

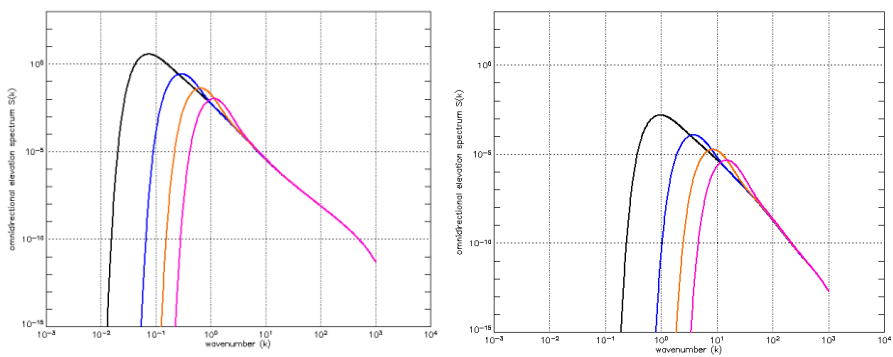


Slide 115  
of 198



# Littoral environments

wind speed 11.5 ms<sup>-1</sup>;  
inverse wave ages 1 to 4

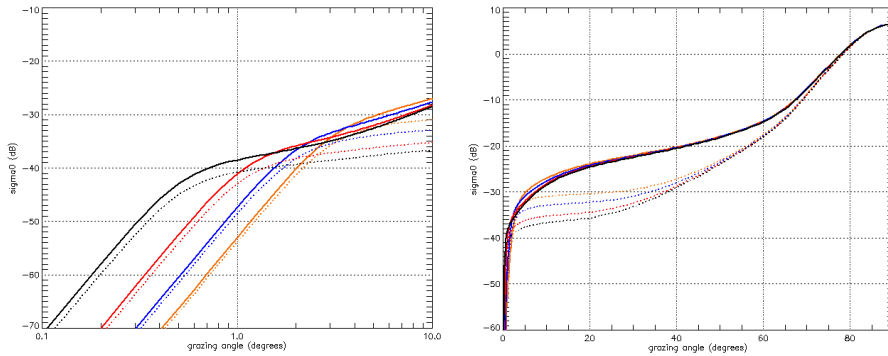


Slide 116  
of 198



# Littoral environments

**Limited fetch at wind speed  $7.6 \text{ ms}^{-1}$ , VV and HH;  
Inverse wave ages 1,2,3 and 4**

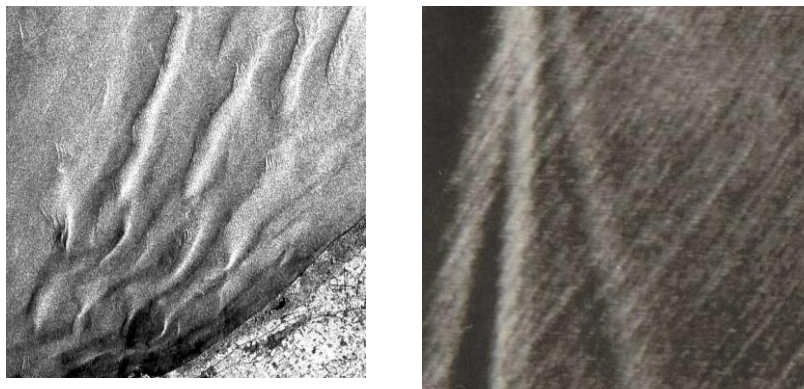


Slide 117  
of 198



# Littoral environments

## (2) Variation of current



Slide 118  
of 198

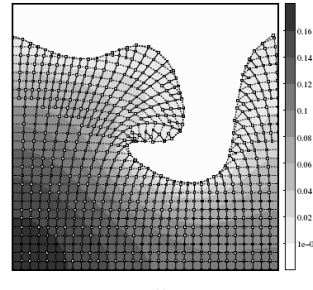


# Littoral environments

## (3) Wave refraction

Ray tracing (Fermat's principle)  
Conservation of energy

*(Figure from: 'An accurate model for wave refraction over shallow water', Gamito and Musgrave)*



Slide 119  
of 198



# Littoral environments

## (4) Breaking in shallow water

Superposition of sinusoids is not sufficient  
Therefore extend model to superposition of 'choppy' waves



Slide 120  
of 198



# Littoral environments

## Gerstner waves

$(x, y)$  particle position at rest

$(\psi_x, \psi_y)$  particle position at time t

$$\psi_x(x, y) = R(y) \sin(\omega t - kx) + x$$

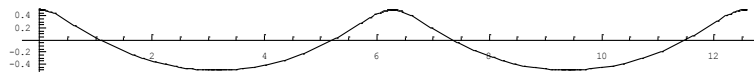
$$\psi_y(x, y) = R(y) \cos(\omega t - kx)$$

$$\omega^2 = gk$$

Water moves up and down and side to side (horizontal advection)

Circular motion in deep water, exponential decay with depth

Breaking criterion can be expressed as the horizontal advection exceeding half the wave phase speed



Slide 121  
of 198



# Littoral environments

## As waves move to shallow water:

They keep the same frequency

The wavelength decreases

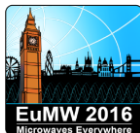
The wave speed decreases

The wave amplitude increases

Particle motions are ellipses rather than circles



Slide 122  
of 198



# Littoral environments

$$\psi_x(x, y) = \frac{a \cosh(k(h+y))}{\sinh(kh)} \sin(\omega t - kx) + x$$

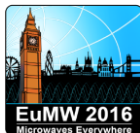
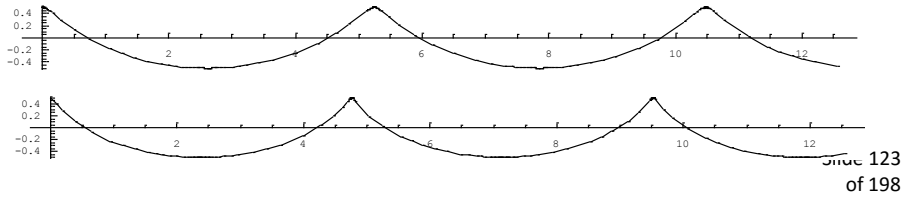
$$\psi_y(x, y) = \frac{a \sinh(k(h+y))}{\sinh(kh)} \cos(\omega t - kx)$$

$$\omega^2 = gk \tanh(kh)$$

**Peak horizontal advection at surface**  $v_{adv} = a\omega \coth(kh)$

**Wave phase velocity**  $v_p = \frac{g}{\omega} \tanh(kh)$

**Breaking criterion**  $\frac{v_{adv}}{v_p} > \frac{1}{2}$  i.e.  $\frac{ak}{\tanh(kh)} > \frac{1}{2}$



# Littoral environments

## Shallow water breaking

**Energy density of a wave is**  $\frac{1}{2} \rho g a^2$

**Energy flux is**  $\frac{1}{2} \rho g a^2 v_g$  and this is constant

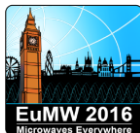
A wave starting in deep water with amplitude  $a_0$  and spatial frequency  $k_0$  changes to  $a$  and  $k$  at depth  $h$

$$k_0 = k \tanh(kh) \quad a_0^2 = a^2 (\tanh(kh) + kh \operatorname{sech}^2(kh))$$

This single wave then breaks if  $\frac{ak}{\tanh(kh)} > \frac{1}{2}$

The addition of many wave components for the full wave spectrum may be analysed through the Jacobian of the transformation from sinusoidal to Gerstner waves (extending the ideas introduced by Tessendorf)

Slide 124  
of 198

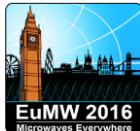


# Littoral environments

## Application

- Having modelled these four littoral effects, i.e.,
  - Change of wave spectrum due to limited fetch
  - Change of wave spectrum due to local current variation
  - Wave refraction due to depth changes
  - Increased breaking due to shallow water
- We are developing a tool to apply the model to specific scenarios (topography, weather conditions) and then predicting radar performance
- Initial results show the types of sensitivity and variation observed in real applications.

Slide 125  
of 198



# Simulation conclusion

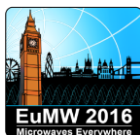
Radar clutter simulation can be done at a number of different levels

- Electromagnetic simulation
- Statistical simulation
- Simulation of the output of radar processing

The results can be used to simulate and emulate radar systems for use throughout their lifecycle

It is important to model the environment and scenario accurately, and to incorporate the effects of these in the sea clutter simulation

Slide 126  
of 198



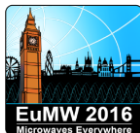
# Coherent Detection in Gaussian and Compound-Gaussian Clutter

Maria S. Greco

University of Pisa

m.greco@iet.unipi.it

Slide 127  
of 198



## Coherent Radar Detection

- ❖ The general radar detection problem
- ❖ Coherent detection in Gaussian clutter
- ❖ Coherent detection in Compound-Gaussian clutter
- ❖ Adaptive detection in Gaussian and compound-Gaussian clutter
- ❖ Final remarks

Slide 128  
of 198



## Coherent Radar Detection

The radar transmits a coherent train of  $m$  pulses and the receiver properly demodulates, filters and samples the incoming narrowband waveform. The samples of the baseband complex signal (in-phase and quadrature components) are:

$$\mathbf{z} = \mathbf{z}_I + j\mathbf{z}_Q = [z[1] \cdots z[m]]^T$$

**Binary hypothesis test:**

$$\begin{cases} H_0: & \mathbf{z} = \mathbf{d} \\ H_1: & \mathbf{z} = \mathbf{s} + \mathbf{d} \end{cases}$$

$\mathbf{s}$  = target signal vector

- Perfectly known;
- Unknown:
  - ✓ deterministic (unknown parameters, e.g., amplitude, initial phase, Doppler frequency, Doppler rate, DOA, etc.)
  - ✓ random (rank-one waveform, multi-dimensional waveform)

**Target samples:**

$$s[n] = A[n]e^{j\vartheta[n]}p[n]$$

$\mathbf{p}$  is the "steering vector"

$$\mathbf{p} = [p[1] \ p[2] \cdots p[m]]^T$$

Slide 129  
of 198



## Gaussian Case: Optimal Detector

The complex multidimensional PDF of Gaussian disturbance is given by:

$$p_{\mathbf{z}|H_0}(\mathbf{z}|H_0) = p_{\mathbf{d}}(\mathbf{z}) = \frac{1}{\pi^m |\mathbf{R}|} \exp(-\mathbf{z}^H \mathbf{R}^{-1} \mathbf{z}) \quad \mathbf{z}|H_0 \in \mathcal{CN}(\mathbf{0}, \mathbf{R})$$

$mx1$  data vector

$$|\mathbf{R}| = \det\{\mathbf{R}\}, \quad \mathbf{R} = \mathbf{R}^H \rightarrow \text{Hermitian matrix}$$

The complex multidimensional PDF of *target + disturbance*:  $p_{\mathbf{z}|H_1}(\mathbf{z}|H_1) = ?$

It depends on the target signal model:  $\mathbf{z} = \mathbf{s}_t + \mathbf{d}$

If the target vector  $\mathbf{s}_t$  is deterministic:

$$p_{\mathbf{z}|H_1}(\mathbf{z}|H_1) = p_{\mathbf{z}|H_0}(\mathbf{z} - \mathbf{s}_t | H_0)$$

130/191

Slide 130  
of 198



## Gaussian Case: Optimum Detector

If the target vector is random with known PDF:

$$p_{\mathbf{z}|H_1}(\mathbf{z}|H_1) = E_{\mathbf{s}_t} \left\{ p_{\mathbf{z}|H_0}(\mathbf{z} - \mathbf{s}_t | H_0) \right\} = \underbrace{\int \frac{1}{\pi^m |\mathbf{R}|} \exp\left(-(\mathbf{z} - \mathbf{s}_t)^H \mathbf{R}^{-1} (\mathbf{z} - \mathbf{s}_t)\right)}_{p_{\mathbf{z}|H_0}(\mathbf{z} - \mathbf{s}_t | H_0)} \cdot p_{\mathbf{s}_t}(\mathbf{s}_t) d\mathbf{s}_t$$

Model for the target signal:

$$\mathbf{s}_t = \beta \mathbf{v}(\nu_d) \quad [\beta \equiv \alpha_r \text{ is the target complex amplitude}]$$

$$\mathbf{s}(\nu_d) = \begin{bmatrix} 1 \\ e^{j2\pi\nu_d} \\ \vdots \\ e^{j2\pi(M-1)\nu_d} \end{bmatrix}$$

Temporal Steering Vector

The waveform PRF is uniform and target velocity is considered constant during the CPI.

Slide 131  
of 198



## Target Signal Models

Different models of  $\mathbf{s}_t$  have been investigated to take into account different degrees of *a priori* knowledge on the target signal:

- (1)  $\mathbf{s}_t$  perfectly known
- (2)  $\mathbf{s}_t = \beta \mathbf{v}$  with  $\beta \in \mathcal{CN}(0, \sigma_s^2)$ , i.e., Swerling I model, and  $\mathbf{v}$  perfectly known;
- (3)  $\mathbf{s}_t = \beta \mathbf{v}$  with  $|\beta|$  deterministic and  $\angle\beta$  random, uniformly distributed in  $[0, 2\pi]$ ,  
i.e. Swerling 0 (or Swerling V) model, and  $\mathbf{v}$  perfectly known
- (4)  $\mathbf{s}_t = \beta \mathbf{v}$  with  $\beta$  unknown deterministic and  $\mathbf{v}$  perfectly known;
- (5)  $\mathbf{s}_t = \beta \mathbf{v}$  with  $\beta$  unknown (deterministic or random) and  $\mathbf{v}$  known function  
of unknown parameters: DOA, Doppler frequency, Doppler rate, etc.
- (6)  $\mathbf{s}_t$  complex Gaussian random vector (known to belong to a subspace of dim.  $r$ ):  

$$\mathbf{s}_t \in \mathcal{CN}\left(0, \sigma_s^2 \mathbf{R}_s\right), \quad r = \text{rank}(\mathbf{R}_s) \leq m, \quad [\mathbf{R}_s]_{i,i} = 1 \forall i$$

of 198



## Perfectly Known Target Signal

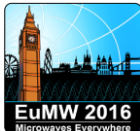
The optimal NP decision strategy is a LRT (or log-LRT):

$$T(\mathbf{z}) = \Re e \left\{ \mathbf{s}_t^H \mathbf{R}^{-1} \mathbf{z} \right\}_{H_0}^{H_1} > \eta$$

It is the so-called coherent whitening matched filter (CWMF) detector:

$$\begin{aligned} \mathbf{s}_t^H \mathbf{R}^{-1} \mathbf{z} &= \mathbf{s}_t^H \mathbf{R}^{-1/2} \mathbf{R}^{-1/2} \mathbf{z} = \mathbf{s}_t^H (\mathbf{R}^{-1/2})^H \mathbf{R}^{-1/2} \mathbf{z} = (\mathbf{R}^{-1/2} \mathbf{s}_t)^H \mathbf{R}^{-1/2} \mathbf{z} = \bar{\mathbf{s}}_t^H \bar{\mathbf{z}} \\ \bar{\mathbf{s}}_t \square \mathbf{R}^{-1/2} \mathbf{s}_t, \quad \bar{\mathbf{z}} \square \mathbf{R}^{-1/2} \mathbf{z} &\text{ whitening transformation} \\ E\{\bar{\mathbf{z}} \bar{\mathbf{z}}^H\} &= E\{\mathbf{R}^{-1/2} \mathbf{z} \mathbf{z}^H \mathbf{R}^{-1/2}\} = \mathbf{R}^{-1/2} E\{\mathbf{z} \mathbf{z}^H\} \mathbf{R}^{-1/2} = \mathbf{R}^{-1/2} \mathbf{R} \mathbf{R}^{-1/2} = \mathbf{I} \end{aligned}$$

Slide 133  
of 198



## Performance Metrics

- To compare the performance of different non-adaptive algorithms with each other, as well as with adaptive approaches, it is necessary to use some standard benchmarks.
- Important radar performance metrics are the probability of detecting a target ( $P_D$ ), the probability of declaring a false alarm ( $P_{FA}$ ), and the accuracy with which target speed and/or bearing may be measured.
- Useful intermediate quantities for the probability of detection are the signal-to-clutter power ratio (SCR) and SCR loss (defined later on).
- Minimum Detectable Velocity. The width of the SINR loss notch near mainlobe clutter determines the lowest velocity detectable by the radar.
- Finally, the response of filter  $\mathbf{w}$  itself is important: it should have a distinct mainlobe that is as narrow as possible as well as low sidelobes.

Slide 134  
of 198



## Performance of the coherent WMF

$$T(\mathbf{z}) = \Re e \left\{ \mathbf{s}_t^H \mathbf{R}^{-1} \mathbf{z} \right\}_{H_0}^{H_1} > \eta$$

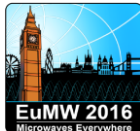
The probability of detection ( $P_D$ ) and probability of false alarm ( $P_{FA}$ ) can be easily calculated

$$P_{FA} = Q \left( \frac{\eta + \mathbf{s}_t^H \mathbf{R}^{-1} \mathbf{s}_t}{\sqrt{2 \mathbf{s}_t^H \mathbf{R}^{-1} \mathbf{s}_t}} \right) \quad P_D = Q \left( \frac{\eta - \mathbf{s}_t^H \mathbf{R}^{-1} \mathbf{s}_t}{\sqrt{2 \mathbf{s}_t^H \mathbf{R}^{-1} \mathbf{s}_t}} \right) = Q \left( Q^{-1}(P_{FA}) - \sqrt{2 \mathbf{s}_t^H \mathbf{R}^{-1} \mathbf{s}_t} \right)$$

where

$$2 \mathbf{s}_t^H \mathbf{R}^{-1} \mathbf{s}_t = SCR_{CWMF}$$

Slide 135  
of 198



## Swerling I Target Signal

$$\mathbf{s}_t = \beta \mathbf{v}(\nu_d), \quad \beta \in \mathcal{CN}(0, \sigma_s^2), \quad \mathbf{v} \text{ perfectly known}$$

$\mathbf{v}$  perfectly known means: array perfectly calibrated, I & Q channels perfectly matched (i.e. balanced), and we are testing for the presence of a target in a given DOA and Doppler frequency bin.

$$\beta = |\beta| e^{j\varphi} \in \mathcal{CN}(0, \sigma_s^2) \Rightarrow |\beta| \text{ is Rayleigh distributed}, E\{|\beta|^2\} = \sigma_s^2 \\ \varphi \text{ is uniformly distributed on } [0, 2\pi)$$

Based upon these assumptions, the optimum NP detector is:

$$|\mathbf{v}^H \mathbf{R}^{-1} \mathbf{z}|^2_{H_0}^{H_1} > \eta$$

Slide 136  
of 198



## Swerling I Target Signal

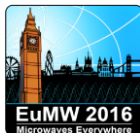
Again, the optimal decision strategy requires calculation of the WMF output, but instead of taking the real part of the output we calculate the modulus of the output: this is due to the fact that the initial target phase in this case is unknown.

This is sometimes termed the noncoherent WMF (a.k.a. the Brennan and Reed test).

$$P_D = (P_{FA})^{\frac{1}{1+SINR_{WMF}}}$$

$$SCR_{WMF} = \sigma_s^2 \mathbf{v}^H \mathbf{R}^{-1} \mathbf{v}$$

Slide 137  
of 198



## Deterministic Unknown Complex Amplitude

$$\Lambda(\mathbf{z}; \beta) = \frac{p_{\mathbf{z}|H_1}(\mathbf{z}|H_1; \beta)}{p_{\mathbf{z}|H_0}(\mathbf{z}|H_0)} \stackrel{H_1}{>} e^\eta \quad \stackrel{H_0}{<} e^\eta$$

The LRT depends on the unknown complex target amplitude, therefore it cannot be implemented.

- This is a composite hypothesis testing problem.
- A uniformly most powerful (UMP) test does not exist.
- We resort to the generalized likelihood ratio test (GLRT) → the unknown parameters are replaced by their maximum likelihood estimates (MLE).

$$\Lambda_{GLRT}(\mathbf{z}) = \max_{\beta} \Lambda(\mathbf{z}; \beta) = \frac{\max_{\beta} p_{\mathbf{z}|H_1}(\mathbf{z}|H_1; \beta)}{p_{\mathbf{z}|H_0}(\mathbf{z}|H_0)} = \frac{p_{\mathbf{z}|H_1}(\mathbf{z}|H_1; \hat{\beta}_{ML})}{p_{\mathbf{z}|H_0}(\mathbf{z}|H_0)} \stackrel{H_1}{>} e^\eta \quad \stackrel{H_0}{<} e^\eta$$

38  
of 198



## Deterministic Unknown Complex Amplitude

$$\hat{\beta}_{ML} = \frac{\mathbf{v}^H \mathbf{R}^{-1} \mathbf{z}}{\mathbf{v}^H \mathbf{R}^{-1} \mathbf{v}}$$

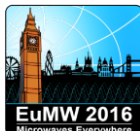
- As a consequence we find the GLRT to be:

$$\ln \Lambda_{GLRT}(\mathbf{z}) = \ln \frac{p_{\mathbf{z}|H_1}(\mathbf{z}|H_1; \hat{\beta}_{ML})}{p_{\mathbf{z}|H_0}(\mathbf{z}|H_0)} = \frac{|\mathbf{v}^H \mathbf{R}^{-1} \mathbf{z}|^2}{\mathbf{v}^H \mathbf{R}^{-1} \mathbf{v}} \stackrel{H_1}{>} \eta \stackrel{H_0}{<} \eta$$

- Incorporating the denominator in the threshold, again we find that the decision strategy is to compare the modulo-squared WMF output to a threshold:

$$|\mathbf{v}^H \mathbf{R}^{-1} \mathbf{z}|^2 \stackrel{H_1}{>} \eta \stackrel{H_0}{<} \eta$$

Slide 139  
of 198



## The Normalized Matched Filter (NMF)

- If the target complex amplitude and the disturbance power are unknown deterministic and we apply the GLRT approach, we get the NMF
- It has the Constant False Alarm Rate (CFAR) property, i.e. its  $P_{FA}$  does not depend on the unknown disturbance power  $\sigma^2$ .

$$\left\{ \begin{array}{l} \hat{\beta}_{ML} = \frac{\mathbf{v}^H \mathbf{M}^{-1} \mathbf{z}}{\mathbf{v}^H \mathbf{M}^{-1} \mathbf{v}} \\ \hat{\sigma}_{ML,0}^2 = \frac{\mathbf{z}^H \mathbf{M}^{-1} \mathbf{z}}{MN} \\ \hat{\sigma}_{ML,1}^2 = \frac{(\mathbf{z} - \hat{\beta}_{ML} \mathbf{v})^H \mathbf{M}^{-1} (\mathbf{z} - \hat{\beta}_{ML} \mathbf{v})}{MN} \end{array} \right.$$

$$\Lambda_{NMF}(\mathbf{z}) = \ln \frac{p_{\mathbf{z}|H_1}(\mathbf{z}|H_1; \hat{\sigma}_{ML,1}^2, \hat{\beta}_{ML})}{p_{\mathbf{z}|H_0}(\mathbf{z}|H_0; \hat{\sigma}_{ML,0}^2)} \equiv \frac{|\mathbf{v}^H \mathbf{M}^{-1} \mathbf{z}|^2}{(\mathbf{v}^H \mathbf{M}^{-1} \mathbf{z})(\mathbf{v}^H \mathbf{M}^{-1} \mathbf{v})} \stackrel{H_1}{>} \eta \stackrel{H_0}{<} \eta$$

Slide 140  
of 198



## Coherent Detection in Compound-Gaussian Clutter

Slide 141  
of 198



### The multidimensional CG model

- Generally, radars process  $M$  pulses at time, thus, to determine the optimal radar processor we need the  **$M$ -dimensional joint PDF**
- Since radar clutter is generally highly correlated, the joint PDF cannot be derived by simply taking the product of the marginal PDFs
- The appropriate multidimensional non-Gaussian model for use in radar detection studies must incorporate the following features:

- 1) it must account for the measured first-order statistics (i.e., the APDF should fit the experimental data)
- 2) it must incorporate pulse-to-pulse correlation between data samples
- 3) it must be chosen according to some criterion that clearly distinguishes it from the multitude of multidimensional non-Gaussian models, satisfying 1) and 2)

Slide 142  
of 198



## The multidimensional CG model

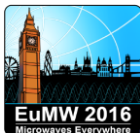
- If the Time-on-Target (ToT) is short, we can consider the texture as constant for the entire ToT, then the compound-Gaussian model degenerates into the spherically invariant random process (**SIRP**)
- By sampling a SIRP we obtain a spherically invariant random vector (**SIRV**) whose PDF is given by

$$p_z(\mathbf{z}) = \frac{1}{(\pi\tau)^M |\mathbf{M}|} \exp\left(-\frac{\mathbf{z}^H \mathbf{M}^{-1} \mathbf{z}}{\tau}\right) p_\tau(\tau) d\tau$$

where  $\mathbf{z} = [z_1 \ z_2 \ \dots \ z_M]^T$  is the  $M$ -dimensional complex vector representing the observed data.

- A random process that gives rise to such a multidimensional PDF can be physically interpreted in terms of a locally Gaussian process whose power level  $\tau$  is random.
- The PDF of the local power  $\tau$  is determined by the fluctuation model of the number  $N$  of scatterers.

Slide 143  
of 198



## Properties of a SIRV

The PDF of a SIRV is a function of a non negative quadratic form:

$$q(\mathbf{z}) = (\mathbf{z} - \mathbf{m}_z)^H \mathbf{M}^{-1} (\mathbf{z} - \mathbf{m}_z)$$

A SIRV is a random vector whose PDF is uniquely determined by the specification of a mean vector  $\mathbf{m}_z$ , a covariance matrix  $\mathbf{M}$ , and a characteristic first-order PDF  $p_\tau(t)$ :

$$p_z(\mathbf{z}) = \frac{1}{(\pi)^M |\mathbf{M}|} h_M(q(\mathbf{z}))$$

$h_M(q)$  must be positive and monotonically decreasing

$$h_M(q) = \int_0^\infty \tau^{-M} \exp\left(-\frac{q}{\tau}\right) p_\tau(\tau) d\tau$$

First-order amplitude PDF:  $p_R(r) = \frac{r}{\sigma^2} h_1\left(\frac{r^2}{\sigma^2}\right), \ \sigma^2 = E\{R^2\} = E\{|z|^2\}$

A SIRV is invariant under a linear transformation: if  $\mathbf{z}$  is a SIRV with characteristic PDF  $p_z(\tau)$ , then  $\mathbf{y} = \mathbf{A}\mathbf{z} + \mathbf{b}$  is a SIRV with the same characteristic PDF  $p_z(\tau)$ .

Slide 144  
of 198



## Properties of a SIRV

Many known APDFs belong to the SIRV family:

Gaussian, Contaminated normal, Laplace, Generalized Laplace, Chauchy, Generalized Chauchy, K, Student-t, Chi, Generalized Rayleigh, Weibull, Rician, Nakagami-m. The log-normal can **not** be represented as a SIRV

for some of them  $p_t(t)$  is not known in closed form

- The assumption that, during the time that the  $m$  radar pulses are scattered, the number  $N$  of scatterers remains fixed, implies that the texture  $t$  is constant during the coherent processing interval (CPI), i.e., **completely correlated texture**
- A more general model is given by  $\zeta[n] = \sqrt{\tau[n]} x[n], n = 1, 2, \dots, m.$
- Extensions to describe the clutter process (instead of the clutter vector), investigated the **cyclostationary** properties of the texture process  $t[n]$

Slide 145  
of 198



## Coherent detection in compound-Gaussian clutter

**The optimum N-P detector is the LLRT:**  $\ln \Lambda(\mathbf{z}) = \ln \frac{p_{\mathbf{z}|H_1}(\mathbf{z}|H_1)}{p_{\mathbf{z}|H_0}(\mathbf{z}|H_0)} \stackrel{H_1}{>} T \stackrel{H_0}{<} T$

$$p_{\mathbf{z}}(\mathbf{z}|H_0) = p_{\mathbf{d}}(\mathbf{z}) = \int_0^{+\infty} \frac{1}{(\pi\tau)^m |\mathbf{M}|} \exp\left[-\frac{q_0(\mathbf{z})}{\tau}\right] p_{\tau}(\tau) d\tau, \quad p_{\mathbf{z}}(\mathbf{z}|H_1) = ?$$

$\mathbf{M}$  is the normalized clutter (speckle) covariance matrix

$$q_0(\mathbf{z}) = \mathbf{z}^H \mathbf{M}^{-1} \mathbf{z}$$

It depends on the target signal model

$$p_{\mathbf{z}}(\mathbf{z}|H_1) = E_s \{ p_{\mathbf{z}}(\mathbf{z} - \mathbf{s}|H_0) \}$$

Slide 146  
of 198



## Deterministic Unknown Complex Amplitude

$$\max_{\beta} \Lambda(\mathbf{z}; \beta) = \Lambda(\mathbf{z}; \hat{\beta}_{ML}) = \frac{p_z(\mathbf{z} - \hat{\beta}_{ML}\mathbf{p} | H_0)}{p_z(\mathbf{z} | H_0)} \stackrel{H_1}{>} e^T \stackrel{H_0}{<}$$

The test statistic is given by the LR for known  $\beta$ , in which the unknown parameter has been replaced by its **maximum likelihood (ML)** estimate

$$\int_0^{+\infty} \frac{1}{\tau^m} \left[ \exp\left(-\frac{q_1(\mathbf{z})}{\tau}\right) - \exp\left(T - \frac{q_0(\mathbf{z})}{\tau}\right) \right] p_\tau(\tau) d\tau \stackrel{H_1}{>} 0 \stackrel{H_0}{<} 0$$

When the number  $m$  of integrated samples increases  $\hat{\beta}_{ML} \rightarrow \beta$ , we expect the GLRT performance to approach that of the NP detector for known signal

$$q_1(\mathbf{z}) = (\mathbf{z} - \hat{\beta}_{ML}\mathbf{p})^H \mathbf{M}^{-1} (\mathbf{z} - \hat{\beta}_{ML}\mathbf{p}) = \mathbf{z}^H \mathbf{M}^{-1} \mathbf{z} - \frac{|\mathbf{p}^H \mathbf{M}^{-1} \mathbf{z}|^2}{\mathbf{p}^H \mathbf{M}^{-1} \mathbf{p}} \text{ where } \hat{\beta}_{ML} = \frac{\mathbf{p}^H \mathbf{M}^{-1} \mathbf{z}}{\mathbf{p}^H \mathbf{M}^{-1} \mathbf{p}}$$

Slide 147  
of 198



## Swerling I Target Signal

The NP detector is given by

$$\Lambda(\mathbf{z}) = \frac{E_\beta \{ p_z(\mathbf{z} - \beta\mathbf{p} | H_0) \}}{p_z(\mathbf{z} | H_0)} \stackrel{H_1}{>} e^T \quad SCR(\tau) = \frac{\sigma_s^2}{\tau}$$

$$\int_0^{+\infty} \frac{1}{\tau^m} \left[ \frac{1}{(1 + SCR(\tau) \cdot \mathbf{p}^H \mathbf{M}^{-1} \mathbf{p})} \exp\left(-\frac{q_1(\mathbf{z})}{\tau}\right) - \exp\left(T - \frac{q_0(\mathbf{z})}{\tau}\right) \right] p_\tau(\tau) d\tau \stackrel{H_1}{>} 0 \stackrel{H_0}{<} 0$$

Interestingly, the structure is similar to the previous one, but now

$$q_1(\mathbf{z}) = \mathbf{z}^H \mathbf{M}^{-1} \mathbf{z} - \frac{SCR(\tau) \cdot |\mathbf{p}^H \mathbf{M}^{-1} \mathbf{z}|^2}{1 + SCR(\tau) \cdot \mathbf{p}^H \mathbf{M}^{-1} \mathbf{p}}$$

Slide 148  
of 198



## Alternative formulation of the OD: the Data-Dependent Threshold

**First step:** express the PDFs under the two hypotheses as:

$$p_z(\mathbf{z}|H_i) = \frac{1}{\pi^m |\mathbf{M}|} h_m(q_i(\mathbf{z})), i = 0, 1$$

where  $\mathbf{h}_m(\mathbf{q})$  is the nonlinear monotonic decreasing function:

$$h_m(q) = \int_0^\infty \frac{1}{\tau^m} \exp\left(-\frac{q}{\tau}\right) p_\tau(\tau) d\tau$$

The LRT can be recast in the form:

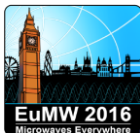
$$q_0(\mathbf{z}) - q_1(\mathbf{z}) \stackrel{H_1}{>} \stackrel{H_0}{<} f_{opt}(q_0, T)$$

$f(\mathbf{q}_0, T)$  is the DDT, that depends on the data only by means of the quadratic statistic

$$f_{opt}(q_0, T) = q_0 - h_m^{-1}(e^T h_m(q_0))$$

$$q_0(\mathbf{z}) = \mathbf{z}^H \mathbf{M}^{-1} \mathbf{z}$$

Slide 149  
of 198



## Alternative formulation of the OD: the Data-Dependent Threshold

$$\text{Gaussian clutter: } q_0(\mathbf{z}) - q_1(\mathbf{z}) \stackrel{H_1}{<} \stackrel{H_0}{>} \sigma_G^2 T$$

$$\text{C-G clutter: } q_0(\mathbf{z}) - q_1(\mathbf{z}) \stackrel{H_1}{>} \stackrel{H_0}{<} f_{opt}(q_0, T)$$

In this formulation the LRT for CG clutter has a similar structure of the OD in Gaussian disturbance, but now the test threshold is not constant but it depends on the data through  $\mathbf{q}_0$

### Perfectly known signal $\mathbf{s}$

(case 1): the OD can be interpreted as the classical whitening-matched filter (WMF) compared to a **data-dependent threshold (DDT)**

$$2 \underbrace{\operatorname{Re} \left\{ \mathbf{s}^H \mathbf{M}^{-1} \mathbf{z} \right\}}_{WMF} \stackrel{H_1}{>} \stackrel{H_0}{<} \mathbf{s}^H \mathbf{M}^{-1} \mathbf{s} + f_{opt}(q_0, T)$$

Slide 150  
of 198



## Alternative formulation of the OD: the Data-Dependent Threshold

### Signal s with unknown

**complex amplitude:** the GLRT again can be interpreted as the classical whitening-matched filter (WMF) compared to the same DDT

$$\underbrace{\left| \mathbf{p}^H \mathbf{M}^{-1} \mathbf{z} \right|^2}_{\text{WMF}} \stackrel{H_1}{>} \stackrel{H_0}{<} \mathbf{p}^H \mathbf{M}^{-1} \mathbf{p} \cdot f_{opt}(q_0, T)$$

Similar results does not hold for the NP detector for Swerling I target signal!

### Example: K-distributed clutter.

In this case the texture is modelled as a Gamma random variable with mean value  $m$  and order parameter  $n$ . For  $v-m=0.5$  we have

$$f_{opt}(q_0, T) = q_0 - \left( \sqrt{q_0} - T \sqrt{\frac{\mu}{4v}} \right)^2 u \left( \sqrt{q_0} - T \sqrt{\frac{\mu}{4v}} \right)$$

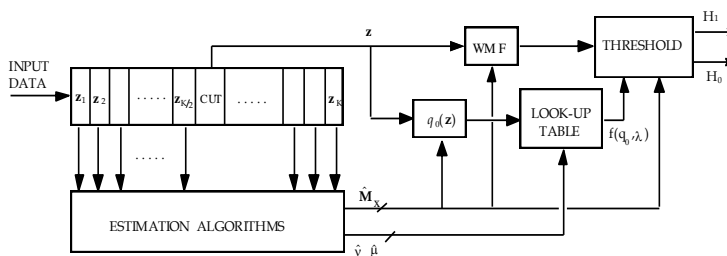
In general, it is not possible to find a closed-form expression for the DDT, so it must be calculated numerically.

Slide 151  
of 198



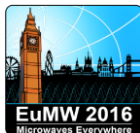
## Canonical structure of the optimum detector

- This **canonical structure** suggests a practical way to implement the OD/GLRT
- The DDT can be a priori tabulated, with  $\lambda$  set according to the prefixed  $P_{FA}$ , and the generated look-up table saved in a memory.



- This approach is highly time-saving, it is canonical for every SIRV, and is useful both for practical implementation of the detector and for performance analysis by means of Monte Carlo simulation
- This formulation provides a deeper insight into the operation of the OD/GLRT and suggests an approach for deriving good suboptimum detectors

Slide 152  
of 198



## Suboptimum detection structures

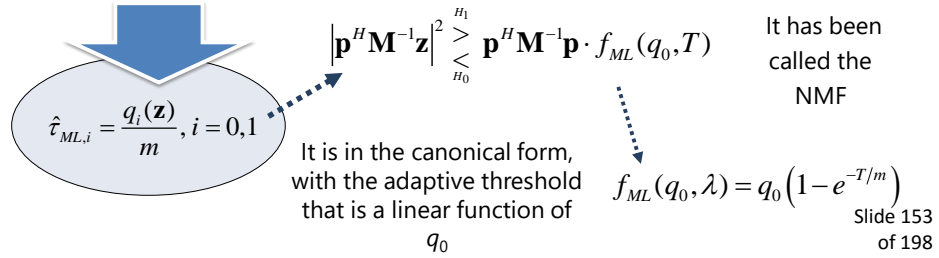
From a physical point of view, the difficulty in utilizing the LR arises from the fact that the power level  $\tau$ , associated with the conditionally Gaussian clutter is unknown and randomly varying: we have to resort to numerical integration

- The **idea** is: replace the unknown power level  $\tau$  with an estimate inside the LR

### Candidate estimation techniques:

MMSE, MAP, ML  
The simplest is the ML

$$\ln \hat{\Lambda}(\mathbf{z}) = m \ln \left( \frac{\hat{\tau}_0}{\hat{\tau}_1} \right) + \frac{q_0(\mathbf{z})}{2\hat{\tau}_0} - \frac{q_1(\mathbf{z})}{2\hat{\tau}_1} \stackrel{H_1}{>} T \stackrel{H_0}{<} T$$



It is in the canonical form, with the adaptive threshold that is a linear function of  $q_0$



## The Normalized Matched Filter (NMF) or GLRT-LQ

$$\frac{|\mathbf{p}^H \mathbf{M}^{-1} \mathbf{z}|^2}{\mathbf{z}^H \mathbf{M}^{-1} \mathbf{z}} \stackrel{H_1}{>} \left(1 - e^{-T/m}\right) \cdot (\mathbf{p}^H \mathbf{M}^{-1} \mathbf{p})$$

- This detector is very simple to implement
- It has the constant false alarm rate (CFAR) property with respect to the clutter PDF

$$P_{FA} = e^{-\frac{T(m-1)}{m}}$$

$$P_D = \int_0^{+\infty} \left( 1 + \frac{\tau(e^{T/m} - 1)}{\tau + m\mu\bar{\gamma}} \right)^{-(m-1)} p_\tau(\tau) d\tau$$

$$\mu = E\{\tau\}$$

$\bar{\gamma} = \frac{\sigma_s^2}{\mu} \cdot \frac{\mathbf{p}^H \mathbf{M}^{-1} \mathbf{p}}{m}$  is the SCR at the output of the WMF, divided by  $m$

Slide 154 of 198



## Suboptimum approximations to the DDT structure

$$\underbrace{\left| \mathbf{p}^H \mathbf{M}^{-1} \mathbf{z} \right|^2}_{WMF} \stackrel{H_1}{<} \stackrel{H_0}{\leq} \mathbf{p}^H \mathbf{M}^{-1} \mathbf{p} \cdot f_{opt}(q_0, T)$$

the threshold  $f(q_0, T)$   
depends in a complicated  
non linear fashion on the  
quadratic statistic  $q_0(\mathbf{z})$

- The **idea** is to find a good approximation of  $f(q_0, T)$  easy to implement.  
In this way, we avoid the need of saving a look-up table in the receiver memory
- The approximation has to be good only for values of  $q_0(\mathbf{z})$  that have a high probability of occurrence
- We looked for the best  **$k$ -th order polynomial approximation** in the MMSE sense

$$f_K(q_0, T) = \sum_{i=0}^K c_i q_0^i$$

$f_K(q_0, T)$  is easy to compute from  $q_0(\mathbf{z})$

$$\min_{\{c_i\}} \left\{ \left| f_{opt}(q_0, T) - \sum_{i=0}^K c_i q_0^i \right|^2 \right\}$$

Slide 155  
of 198



## Suboptimum approximations to the DDT structure

**Example:** First order (linear) approximation:  $f_1(q_0, T) = c_0 + c_1 q_0$

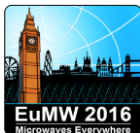
The solution is obtained by solving a  $(K+1)$ -th order linear system. For  $K=1$ :

$$\begin{bmatrix} c_0 \\ c_1 \end{bmatrix} = \begin{bmatrix} 1 & E\{q_0\} \\ E\{q_0\} & E\{q_0^2\} \end{bmatrix}^{-1} \begin{bmatrix} E\{f_{opt}(q_0, T)\} \\ E\{q_0 f_{opt}(q_0, T)\} \end{bmatrix}$$

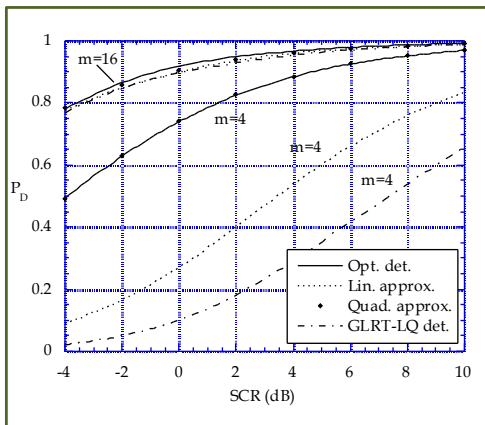
For the 1st (linear)  
and 2nd-order  
(quadratic)  
approximations:

$c_0 \propto \mu$ ,  $c_1$  independent of  $\mu$ ,  $c_2 \propto 1/\mu$   
all  $c_i$ 's are independent of  $\mathbf{M}$

Slide 156  
of 198



## Performance Analysis: Sw-I target, K-distributed clutter

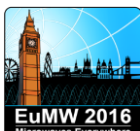


$$P_{FA} = 10^{-5}, f_D = 0.5, \nu = 4.5, \mu = 10^3,$$

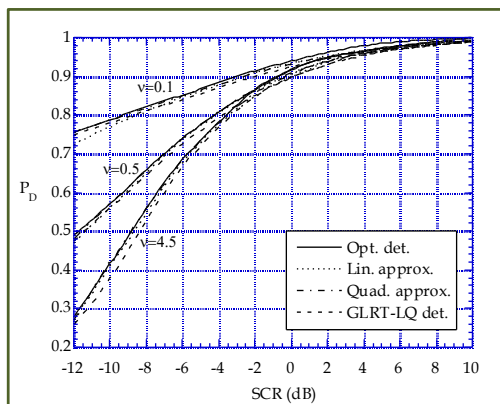
$$\rho_X = 0.9 AR(1)$$

- The detector based on 2<sup>nd</sup>-order approximation represents a good trade-off between performance and ease of implementation
- It requires knowledge of the clutter APDF parameters ( $n$  and  $m$ )
- As the number  $m$  of integrated pulses increases, the detection performance of the GLRT-LQ approaches the optimal performance
- The GLRT-LQ does not require knowledge of  $n$  and  $m$
- It is also CFAR w.r.t. texture PDF

Slide 157  
of 198



## Performance Analysis: Sw-I target, K-distributed clutter

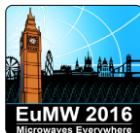


$$P_{FA} = 10^{-5}, f_D = 0.5, m = 16, \mu = 10^3,$$

$$\rho_X = 0.9 AR(1)$$

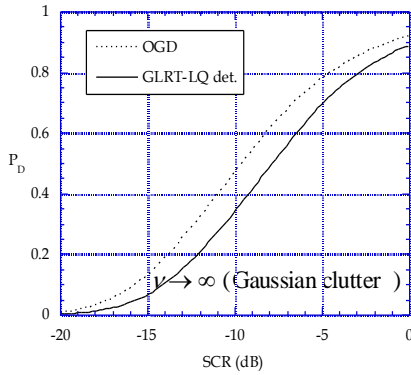
- Clutter spikiness heavily affects detection performance
- $n=0.1$  means very spiky clutter (heavy tailed)
- $n=4.5$  means almost Gaussian clutter
- Up to high values of SCR the best detection performance is obtained for spiky clutter (small values of  $n$ ): it is more difficult to detect weak targets in Gaussian clutter rather than in spiky K-distributed clutter, provided that the proper decision strategy is adopted

Slide 158  
of 198

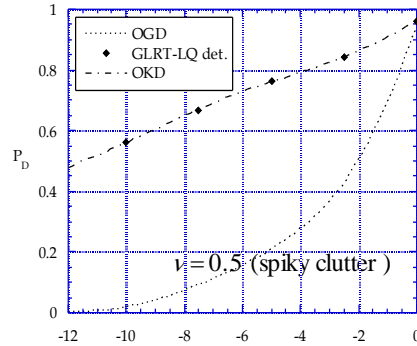


## Performance Analysis: Sw-I target, K-distributed clutter

Optimum Detector in K-clutter (OKD) , Optimum Detector in Gaussian clutter  
(OGD) = whitening matched filter (WMF)



$$P_{FA} = 10^{-5}, f_D = 0.5, m = 16, \mu = 10^3, \rho_X = 0.9 AR(1)$$

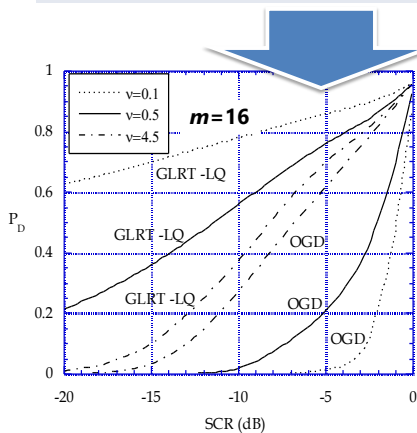


The 2nd figure shows how a wrong assumption on clutter model (model mismatching) affects detection performance ,  
of 198

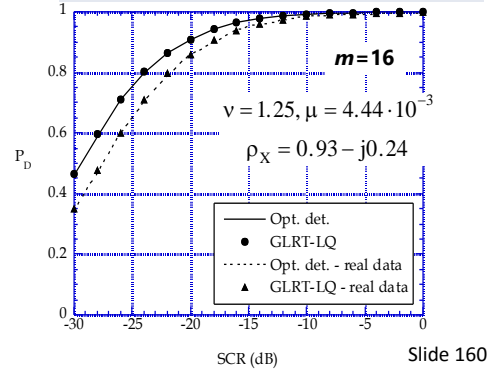


## Swerling-I, K-distributed clutter, real sea clutter data

- The gain of the GLRT-LQ over the mismatched OGD increases with clutter spikiness (decreasing values of n)



- Performance prediction have been checked with **real sea clutter data**
- The detectors make use of the knowledge of m, n, and M (obtained from the entire set of data)



Slide 160  
of 198



## Adaptive Target Detection

Slide 161  
of 198



### Adaptive detection in Gaussian disturbance

- The Optimum and Suboptimum Detectors in previous section have been obtained supposing that the disturbance covariance matrix is a priori known. Most often this is not true and it must be estimated using K secondary data surrounding the CUT.

- We suppose homogeneous environment:

$\mathbf{z}|H_0$  and  $\{\mathbf{z}_k\}_{k=1}^K$  are independent and identically distributed (IID)

$$\mathbf{R} = \sigma^2 \mathbf{M} \quad E\{\mathbf{z}\mathbf{z}^H | H_0\} = E\{\mathbf{z}_k\mathbf{z}_k^H\}, \quad k = 1, 2, \dots, K$$

Slide 162  
of 198



## Disturbance Covariance Matrix Estimation

- The so-called Sample Covariance Matrix (SCM) estimate is obtained by simply replacing statistical averaging with the secondary data vectors sample mean:

$$\hat{\mathbf{R}} = \frac{1}{K} \sum_{k=1}^K \mathbf{z}_k \mathbf{z}_k^H$$

- Property:  $\det(\hat{\mathbf{R}}) \neq 0$  with probability 1 if  $K \geq NM$
- It can be proved that it is also the maximum likelihood (ML) estimate if the disturbance is Gaussian distributed.

Slide 163  
of 198



## The Adaptive Matched Filter (AMF)

- If we plug the SCM estimate in place of the true one in the WMF detector, we get the so-called Adaptive Matched Filter (AMF):

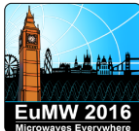
$$\Lambda_{AMF}(\mathbf{z}) = \Lambda_{WMF}(\mathbf{z}) \Big|_{\mathbf{R}=\hat{\mathbf{R}}} = \frac{|\mathbf{v}^H \hat{\mathbf{R}}^{-1} \mathbf{z}|^2}{\mathbf{v}^H \hat{\mathbf{R}}^{-1} \mathbf{v}} \begin{cases} > \eta & H_1 \\ < \eta & H_0 \end{cases}$$

- Note that now the denominator is no more an unessential (non data-dependent) scaling factor. Now it depends on the secondary data.

$$\mathbf{w} = \hat{\mathbf{R}}^{-1} \mathbf{v} \quad \text{data-dependent (adaptive) weights}$$

[Rob92] F. C. Robey, D. L. Fuhrman, E. J. Kelly, and R. Nitzberg, "A CFAR Adaptive Matched Filter Detector," *IEEE Trans. on Aerospace and Electronic Systems*, Vol. 29, No.1, pp. 208-216, January 1992.

Slide 164  
of 198



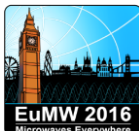
## The Adaptive Normalized Matched Filter (ANMF)

- If we plug the SCM estimate in place of the true one in the NMF detector, we get the so-called Adaptive Normalized Matched Filter (ANMF), a.k.a. Adaptive Coherence Estimator (ACE):

$$\begin{aligned}\Lambda_{ANMF}(\mathbf{z}) &= \Lambda_{NMF}(\mathbf{z})|_{\mathbf{M}=\hat{\mathbf{M}}} = \frac{|\mathbf{v}^H \hat{\mathbf{M}}^{-1} \mathbf{z}|^2}{(\mathbf{z}^H \hat{\mathbf{M}}^{-1} \mathbf{z})(\mathbf{v}^H \hat{\mathbf{M}}^{-1} \mathbf{v})} \\ &= \frac{|\mathbf{v}^H \hat{\mathbf{R}}^{-1} \mathbf{z}|^2}{(\mathbf{z}^H \hat{\mathbf{R}}^{-1} \mathbf{z})(\mathbf{v}^H \hat{\mathbf{R}}^{-1} \mathbf{v})} \stackrel{H_1}{>} \eta \quad \text{where } \hat{\mathbf{R}} = \hat{\sigma}^2 \hat{\mathbf{M}} \\ &\stackrel{H_0}{<} \eta\end{aligned}$$

- The statistic of the test is a measure of the similarity (coherence) between the received data vector and the hypothesized target signal vector, that's why it is also called the Adaptive Coherence Estimator (ACE).

Slide 165  
of 198



## Kelly's GLRT

- The binary hypotheses testing problem is stated as follows:

$$\left\{ \begin{array}{ll} H_0 : \text{Target absent} & \left\{ \begin{array}{l} \mathbf{z} = \mathbf{d} \\ \mathbf{z}_k = \mathbf{d}_k, k = 1, 2, \dots, K \end{array} \right. \\ H_1 : \text{Target present} & \left\{ \begin{array}{l} \mathbf{z} = \beta \mathbf{v} + \mathbf{d} \\ \mathbf{z}_k = \mathbf{d}_k, k = 1, 2, \dots, K \end{array} \right. \end{array} \right.$$

- This is a composite hypotheses testing problem since some parameters are unknown, i.e. the target complex amplitude  $\beta$  and the disturbance covariance matrix  $\mathbf{R}$ .
- For this problem a uniformly most powerful test (UMP) does not exist (an UMP test is a rule that maximizes the  $P_D$  regardless of the unknown parameters of the distribution of the data under  $H_1$ , for a preassigned  $P_{FA}$ ). For this reason we have to resort to the Generalized Likelihood Ratio Test (GLRT).

Slide 166  
of 198



## Kelly's GLRT

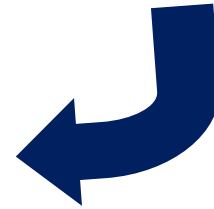
- According to the GLRT approach, we have to calculate the likelihood ratio test (LRT), i.e. the ratio of the PDFs of the data vector under the two hypotheses, and then replace the unknown parameters in each PDF by their Maximum Likelihood (ML) estimates:

$$\Lambda_{GLRT}(\mathbf{z}) = \frac{\max_{\beta, \mathbf{R}} p_{\mathbf{z}|H_1}(\mathbf{z}, \mathbf{z}_1, \mathbf{z}_2, \dots, \mathbf{z}_K; \beta, \mathbf{R} | H_1)}{\max_{\mathbf{R}} p_{\mathbf{z}|H_0}(\mathbf{z}, \mathbf{z}_1, \mathbf{z}_2, \dots, \mathbf{z}_K; \mathbf{R} | H_0)} = \frac{p_{\mathbf{z}|H_1}(\mathbf{z}, \mathbf{z}_1, \mathbf{z}_2, \dots, \mathbf{z}_K; \hat{\beta}_{ML}, \hat{\mathbf{R}}_{ML1} | H_1)}{p_{\mathbf{z}|H_0}(\mathbf{z}, \mathbf{z}_1, \mathbf{z}_2, \dots, \mathbf{z}_K; \hat{\mathbf{R}}_{ML0} | H_0)}$$

where:

$$(\hat{\beta}_{ML}, \hat{\mathbf{R}}_{ML1}) = \arg \max_{\beta, \mathbf{R}} p_{\mathbf{z}|H_1}(\mathbf{z}, \mathbf{z}_1, \mathbf{z}_2, \dots, \mathbf{z}_K; \beta, \mathbf{R} | H_1)$$

$$\hat{\mathbf{R}}_{ML0} = \arg \max_{\mathbf{R}} p_{\mathbf{z}|H_0}(\mathbf{z}, \mathbf{z}_1, \mathbf{z}_2, \dots, \mathbf{z}_K; \mathbf{R} | H_0)$$



Slide 167  
of 198



## Kelly's GLRT

Finally, it can be recast in the well-known form:

$$\Lambda_{GLRT}(\mathbf{z}) = \frac{|\mathbf{v}^H \mathbf{S}^{-1} \mathbf{z}|^2}{(\mathbf{v}^H \mathbf{S}^{-1} \mathbf{v})(1 + \mathbf{z}^H \mathbf{S}^{-1} \mathbf{z})} \stackrel{H_1}{>} \eta \stackrel{H_0}{<} \eta$$

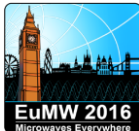
or making explicit the dependence on the SCM:

$$\hat{\mathbf{R}} = \frac{1}{K} \mathbf{S} = \frac{1}{K} \sum_{k=1}^K \mathbf{z}_k \mathbf{z}_k^H$$



$$\Lambda_{GLRT}(\mathbf{z}) = \frac{|\mathbf{v}^H \hat{\mathbf{R}}^{-1} \mathbf{z}|^2}{(\mathbf{v}^H \hat{\mathbf{R}}^{-1} \mathbf{v}) \left(1 + \frac{1}{K} \mathbf{z}^H \hat{\mathbf{R}}^{-1} \mathbf{z}\right)} \stackrel{H_1}{>} \eta \stackrel{H_0}{<} \eta$$

Slide 168  
of 198

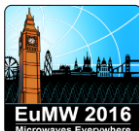


## Kelly's GLRT

- The terms in parentheses at the denominator is computationally intensive for real time systems, as it must be calculated for each new input sample.
- This term tends to unity when  $K$  is large, hence Kelly's GLRT and AMF tends to be the same for large  $K$ .
- It has been proved that Kelly's GLRT outperforms the AMF for small SINRs, instead for high SINRs the AMF usually outperforms the GLRT (this is a confirmation that the GLRT is not a UMP test).
- The absence of the denominator term causes the AMF to be much more sensitive to signals that would appear in the sidelobes of the adapted antenna pattern (mismatched targets), i.e. the AMF is less selective.
- Analytical expressions of AMF, ANMF and Kelly's detector can be found in [Kel86] and [Ban09]

[Kel86] E. J. Kelly, Adaptive Detection Algorithm," *IEEE Trans. on Aerospace and Electronic Systems*, Vol. 22, No.2, pp. 115-127, March 1986.

[Ban09] F. Bandiera, D. Orlando and G. Ricci. "Advanced Radar Detection Schemes Under Mismatched Signal Models". *Synthesis Lectures on Signal Processing*, 2009, Vol.4, No.1, pp. 1-105. Slide 169 of 198



## Adaptive Detection in Compound-Gaussian Clutter

Slide 170  
of 198



## Adaptive detection in CG disturbance

Again, the Optimum and Suboptimum Detectors in previous sections have been obtained supposing that the disturbance covariance matrix is a priori known. Most often this is not true and it must be estimated using K secondary data surrounding the CUT.

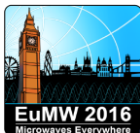
We suppose homogeneous environment:

$\mathbf{z}|H_0$  and  $\{\mathbf{z}_k\}_{k=1}^K$  are independent and identically distributed (IID)

$$\mathbf{R} = \sigma^2 \mathbf{M} \quad E\{\mathbf{z}\mathbf{z}^H|H_0\} = E\{\mathbf{z}_k\mathbf{z}_k^H\} = E\{\tau_k\}E\{\mathbf{x}_k\mathbf{x}_k^H\}, k=1,2,\dots,K$$

$$\mathbf{R}|\tau_k = \tau_k \mathbf{M} \quad E\{\mathbf{z}_k\mathbf{z}_k^H|\tau_k\} = \tau_k E\{\mathbf{x}_k\mathbf{x}_k^H\}, k=1,2,\dots,K$$

Slide 171  
of 198



## Adaptive detection in CG disturbance

- We could resort to the Maximum Likelihood approach where the unknowns are the normalized covariance matrix M, the vector of the textures in the secondary and primary vectors  $\Theta_r = [\tau \ \tau_1 \ \dots \ \tau_K]^T$  and the amplitude  $\alpha$  of the target  $\mathbf{s} = \alpha \mathbf{p}$

$$\frac{\max_{\mathbf{M}, \Theta_r, \alpha} f(Z|H_1)_{H_1}}{\max_{\mathbf{M}, \Theta_r} f(Z|H_0)_{H_0}} \gtrsim \lambda$$

- This approach leads to an infeasible multidimensional non-linear maximization problem for which no closed form seems to exist.
- An alternative approach is to consider the disturbance matrix as known, derive the GLRT and then replace M with an appropriate estimate, resorting to

$$\frac{\left| \mathbf{p}^H \hat{\mathbf{M}}^{-1} \mathbf{z} \right|^2}{(\mathbf{z}^H \hat{\mathbf{M}}^{-1} \mathbf{z})(\mathbf{p}^H \hat{\mathbf{M}}^{-1} \mathbf{p})_{H_0}} \stackrel{H_1}{>} \lambda$$

Slide 172  
of 198



## Covariance matrix estimation approaches

- **Naïve.** We ignore that for some particular CG model the disturbance can present large outliers and we decide to treat it as Complex Gaussian distributed for ease of calculation.
- **Robust.** We ignore again the information on the CG model but we use a particular robust matrix estimator that is not "optimum" for any CG distribution, but independent of any particular CG model and easy to implement.
- **Fully adaptive.** We suppose to know that the disturbance belongs to a particular CG model, characterized by a specific set of parameters whose values are unknown and we jointly estimate all of them together with the covariance matrix.

Slide 173  
of 198



## Naïve approach

Maximum Likelihood (ML) estimator of  $\mathbf{M}$  for Gaussian distributed data, that is the sample covariance matrix estimator (SCM)

$$\hat{\mathbf{M}}_{ML} = \hat{\mathbf{M}}_{SCM} = \frac{1}{\sigma^2 K} \sum_{k=1}^K \mathbf{z}_k \mathbf{z}_k^H$$

Even for compound-Gaussian disturbance, this estimate is unbiased and consistent.

$$E\{\hat{\mathbf{M}}_{SCM}\} = \frac{1}{\sigma^2 K} \sum_{k=1}^K E\{\mathbf{z}_k \mathbf{z}_k^H\} = \frac{1}{K} \sum_{k=1}^K \mathbf{M} = \mathbf{M}$$

$\lim_{K \rightarrow \infty} \hat{\mathbf{M}}_{SCM} = \mathbf{M}$  (convergence in mean square sense)

$$i.e. \quad \lim_{K \rightarrow \infty} E\left\{\left|\mathbf{M}_{i,k} - \hat{\mathbf{M}}_{SCM_{i,k}}\right|^2\right\} = 0$$

Slide 174  
of 198



## Robust approach: the complex Tyler's estimator

$$\hat{\mathbf{M}}_T = \frac{1}{K} \sum_{k=1}^K \frac{\mathbf{z}_k \mathbf{z}_k^H}{\mathbf{z}_k^H \hat{\mathbf{M}}_T^{-1} \mathbf{z}_k} = \frac{1}{K} \sum_{k=1}^K \frac{\mathbf{s}_k \mathbf{s}_k^H}{\mathbf{s}_k^H \hat{\mathbf{M}}_T^{-1} \mathbf{s}_k} \quad \text{where } \mathbf{s}_k = \mathbf{z}_k / \|\mathbf{z}_k\|$$

Each vector  $\mathbf{s}_k$  has a complex angular elliptical (CAE) distribution, no matter what the original CG was and  $\hat{\mathbf{M}}_T$  is the ML scatter matrix for CAE distributed data.

This estimator has been also derived as an approximate ML estimator of the scatter matrix of CG distributed data [Gin02] and it is sometimes called Fixed-Point (FP) estimator [Pas08].

Slide 175  
of 198



## Fully-adaptive approach: known scale and shape parameters

A third possible estimator is the maximum likelihood (ML) one. To derive it we start from the joint pdf of the K secondary vectors with known scale and shape parameters

$$\begin{aligned} p_Z(\mathbf{z}_1, \mathbf{z}_2, \dots, \mathbf{z}_K) &= \prod_{k=1}^K p_z(\mathbf{z}_k) = \prod_{k=1}^K \int_0^\infty p_z(\mathbf{z}_k | \tau_k) p_\tau(\tau_k) d\tau_k \\ &= \prod_{k=1}^K \int_0^{+\infty} \frac{1}{(\pi \tau_k)^M |\mathbf{M}|} \exp\left(-\frac{\mathbf{z}_k^H \mathbf{M}^{-1} \mathbf{z}_k}{\tau_k}\right) p_\tau(\tau_k) d\tau_k \end{aligned}$$

Defining the function  $h_M(q) \triangleq \int_0^{+\infty} \frac{1}{\tau^M} \exp(-q/\tau) d\tau$

$$\rightarrow p_Z(\mathbf{z}_1, \mathbf{z}_2, \dots, \mathbf{z}_K) = \pi^{-KM} |\mathbf{M}|^{-K} \prod_{k=1}^K h_M(\mathbf{z}_k^H \mathbf{M}^{-1} \mathbf{z}_k)$$

Slide 176  
of 198



## Fully-adaptive approach

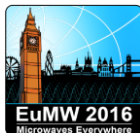
The ML estimator is the solution (if it exists) of a trascendental equation. We can solve it iteratively:

$$\hat{\mathbf{M}}_{ML}(i+1) = \frac{1}{K} \sum_{k=1}^K c_M \left( \mathbf{z}_k^H \hat{\mathbf{M}}_{ML}^{-1}(i) \mathbf{z}_k \right) \cdot \mathbf{z}_k \mathbf{z}_k^H$$

where  $c_M(x) \triangleq h_{M+1}(x)/h_M(x)$

- Calculation of the K data-dependent coefficients  $c_M(\cdot)$  requires knowledge of the texture PDF.
- Even when the texture pdf is perfectly known, the calculation of these coefficients can be too computationally heavy for real time operation.
- The choice of a good starting point to prevent convergence to local maxima.

Slide 177  
of 198



## The ANMF detector with estimated covariance

Let's now plug the disturbance matrix estimators in the ANMF making this detector adaptive to the covariance matrix.

It is important to verify if the new ANMF is CFAR with respect to the true covariance matrix  $\mathbf{M}$ .

For this purpose, we simulate a K-distributed clutter with an AR(1) speckle correlation function  $R_x(l) = \rho^{|l|}$  and shape parameter  $\nu=0.5$ .

Changing the one-lag correlation coefficient  $\rho$  we change the shape of the clutter PSD.

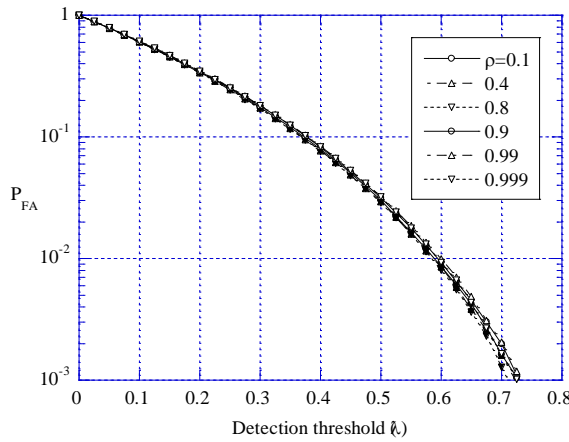
In this simulation the number of integrated pulses in  $N=8$  and the number of secondary vectors is  $K=3N=24$

The Doppler frequency of the target is  $\nu_d=0.15$ .

Slide 178  
of 198

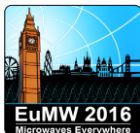


## ANMF-ML

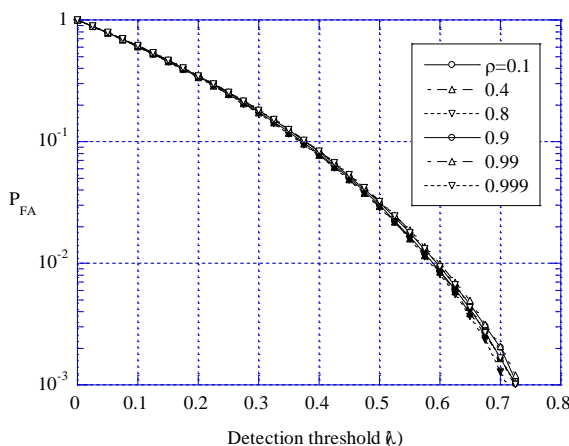


The ANMF-ML is very robust (practically CFAR) with respect to the matrix M.

Slide 179  
of 198

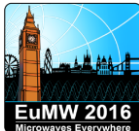


## ANMF-Tyler



The ANMF-Tyler is very robust (practically CFAR) with respect to the matrix M and its performance are very similar to that of the ANMF-ML.

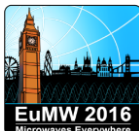
Slide 180  
of 198



## Non-stationary Sea Clutter

### Impact on Disturbance Covariance Matrix Estimate and Detector CFAR property

Slide 181  
of 198



## IPIX Data Description

Data collected at Grimsby, lake Ontario, with McMaster Univ. IPIX radar.

Operational radar parameters:

Transmitter	Receiver	Parabolic dish antenna
TWT peak power: 8 KW	Number of receivers: 2	Diameter: 2.4 m
Dual freq. transmission: 8.9-9.4 GHz	Outputs: Linear, I and Q	Pencil beamwidth (Azim. Res.): 1.1 degrees
H-V polarization, agile	Receiving polariz.: H-V	Antenna gain: 45.7 dB
Pulse width: 20 ns to 5000 ns (real) 5000 ns (expanded) 32 ns (compressed)	Data acquisition: Sample rate: 0 to 50 MHz Outputs: Linear, I, Q Quantization: 10 bit- up to 16 bit effective	Cross-pol. isolation: 30 dB
PRF: from 0 to 20 KHz		Double pol. with central feeder

Slide 182  
of 198



## Sea clutter non-stationarity

A statistical analysis of real data has been performed

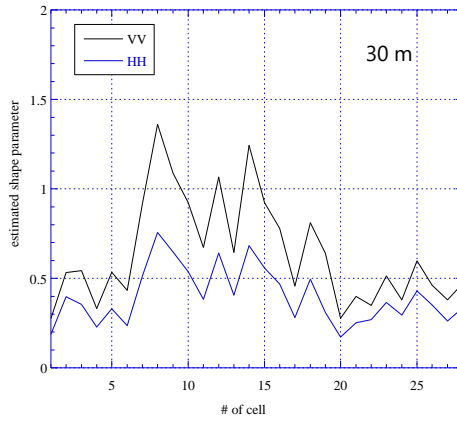


Reasonable fit of the data to the K model.

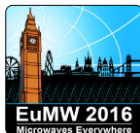
The shape parameter  $\nu$  is not constant on all the range cells



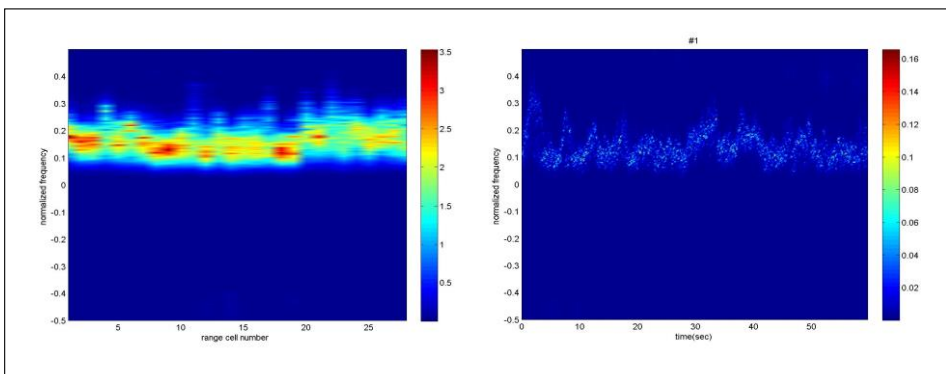
The values of  $\nu$  for the HH data are always lower than those for the VV data. The ratio between the parameters of the VV data and the HH data is close to 0.6 for each cell and each analyzed file.



Slide 183  
of 198



## Sea clutter non-stationarity: VV data



PSD of sea clutter changes from cell to cell  
**Spatial non-stationarity**

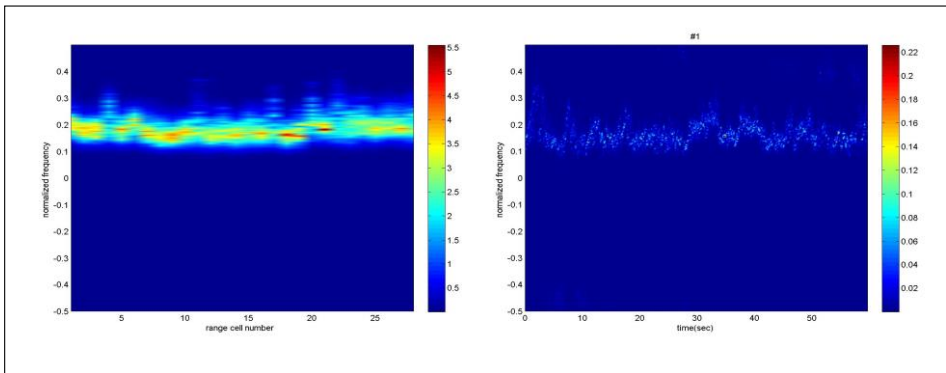
PSD of sea clutter changes in time  
**Temporal non-stationarity**

The peak of the PSD is in the range [0.1, 0.2] but changes with space and time

Slide 184  
of 198



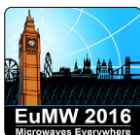
## Sea clutter non-stationarity: HH Data



PSD of sea clutter changes from  
cell to cell  
**Spatial non-stationarity**

**Temporal non-stationarity**  
The PSD exhibits a periodic behavior  
due to the contribution of the long  
waves

Slide 185  
of 198



## Sea clutter non-stationarity

- The sea clutter shows a good fit to K model but the shape parameter of the distribution changes from cell to cell
- The speckle PSD is not constant in time and space. The clutter is not spatially and temporally stationary. The spectrogram evidences some temporal periodicity in spectrum PSD behavior
- Cell under test and secondary vectors do not share same covariance matrix

Slide 186  
of 198



## Adaptive Normalized Matched Filter

The detection of a target signal in additive clutter can be posed in terms of a binary hypotheses test:

$$\begin{cases} H_0 : \mathbf{z} = \mathbf{c} \\ H_1 : \mathbf{z} = \mathbf{s} + \mathbf{c} \end{cases}$$

CUT

$\mathbf{z}_i = \mathbf{c}_i \quad i = 1, \dots, K$

$\mathbf{z}_i = \mathbf{c}_i \quad i = 1, \dots, K$

$\mathbf{s} = \alpha \mathbf{p}$  Swerling I target model

$\alpha \in \mathcal{CN}(0, \sigma_\alpha^2)$

The clutter is modeled as a compound-Gaussian process

$$\mathbf{c} = \sqrt{\tau} \mathbf{x} \quad \mathbf{c}_i = \sqrt{\tau_i} \mathbf{x}_i$$

$$\mathbf{x}, \mathbf{x}_i \in \mathcal{CN}(\mathbf{0}, \mathbf{M})$$

The clutter in the CUT and in the secondary vectors are supposed to share the same statistical properties



ANMF

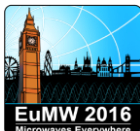
$$\frac{\left| \mathbf{p}^H \hat{\mathbf{M}}^{-1} \mathbf{z} \right|^2}{\left( \mathbf{p}^H \hat{\mathbf{M}}^{-1} \mathbf{p} \right) \left( \mathbf{z}^H \hat{\mathbf{M}}^{-1} \mathbf{z} \right)} \stackrel{H_0}{\ntrianglelefteq} \lambda$$

where

$$\hat{\mathbf{R}} = \hat{\mathbf{R}}(\mathbf{z}_1, \dots, \mathbf{z}_K)$$

$$\mathbf{R} = E\{\mathbf{cc}^H\} = \sigma^2 \mathbf{M}$$

Slide 187  
of 198



## Covariance matrix estimation

Sample covariance matrix (SCM)

$$\hat{\mathbf{M}}_{SCM} = \frac{1}{K} \sum_{i=1}^K \mathbf{z}_i \mathbf{z}_i^H \equiv \frac{1}{K} \sum_{i=1}^K \tau_i (\mathbf{x}_i \mathbf{x}_i^H)$$

ANMF is CFAR with respect to M,  
strongly depends on the pdf of the texture

Normalized sample covariance matrix (NSCM)

$$\hat{\mathbf{M}}_{NSCM} = \frac{N}{K} \sum_{i=1}^K \frac{\mathbf{z}_i \mathbf{z}_i^H}{\mathbf{z}_i^H \mathbf{z}_i} \equiv \frac{N}{K} \sum_{i=1}^K \frac{\mathbf{x}_i \mathbf{x}_i^H}{\mathbf{x}_i^H \mathbf{x}_i}$$

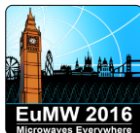
ANMF is CFAR w.r.t. the pdf of the texture,  
but depends on M

Tyler's or fixed point (FP) estimator

$$\hat{\mathbf{M}}_{AML} = \frac{N}{K} \sum_{i=1}^K \frac{\mathbf{z}_i \mathbf{z}_i^H}{\mathbf{z}_i^H \hat{\mathbf{M}}_{AML}^{-1} \mathbf{z}_i} \equiv \frac{N}{K} \sum_{i=1}^K \frac{\mathbf{x}_i \mathbf{x}_i^H}{\mathbf{x}_i^H \hat{\mathbf{M}}_{AML}^{-1} \mathbf{x}_i}$$

ANMF is CFAR w.r.t. the pdf of the texture,  
and very robust w.r.t. M

Slide 188  
of 198



## Performance comparison

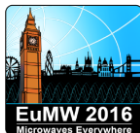
For comparison purposes:

We generated K-distributed clutter with  
covariance matrix equal to the average covariance matrix of  
the measured data  
and shape parameter equal to the estimated  $v_{\text{mean}}$

We set the threshold for a nominal  $P_{\text{FA}0}=10^{-2}$  and  $10^{-3}$  in the  
ANMF with each of the 3 covariance matrix estimators

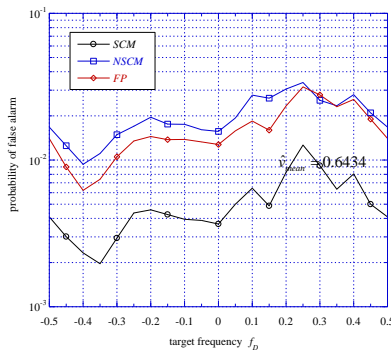
We fed the ANMF with the real data and plot the "true"  $P_{\text{FA}}$

Slide 189  
of 198

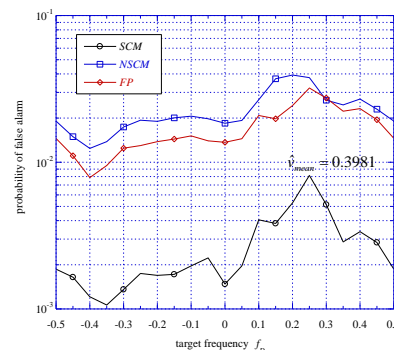


## Performance comparison: $P_{\text{FA}}$

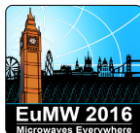
VV data



HH data



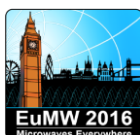
Slide 190  
of 198



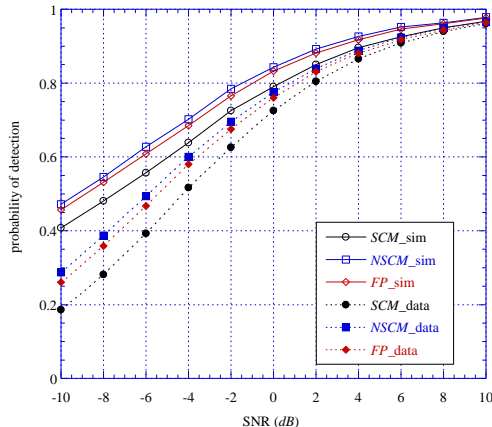
## Performance comparison: $P_{FA}$

- The actual  $P_{FA}$  of NSCM and FP are close to the nominal one for  $f_D$  in the noise floor. For  $f_D$  close to the PSD peak, the real  $P_{FA}$  is higher.
- The actual  $P_{FA}$  of the SCM is almost always lower than the nominal one.
- The deviations are higher where the spectrum variations due to clutter non-stationarity are greater. (It is the peak of the PSD or the Doppler centroid that moves with the long waves originating the almost periodic behavior of the spectrogram).
- The differences in the SCM can be mostly due to the non-stationarity of the shape parameter  $v$ , more than to the non-stationarity of the covariance matrix. The SCM is particularly sensitive to the clutter texture PDF.

Slide 191  
of 198



## Performance comparison: $P_D$



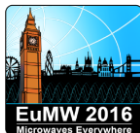
$N=8, K=16, P_{FA0}=10^{-2}$

$f_D=0, \text{VV data}$

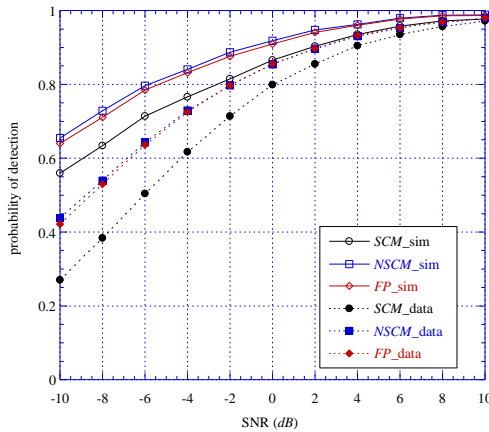
The actual  $P_D$  is always lower than the nominal one for each detector and matrix estimator.

This is always true also in cases where the actual  $P_{FA}$  is higher than the nominal one.

Slide 192  
of 198



## Performance comparison: $P_D$

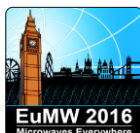


$N=8, K=16, P_{FA0}=10^{-2}$

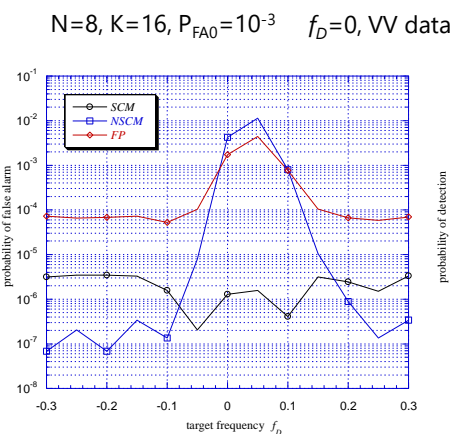
$f_D=0, \text{HH data}$

The non-stationarity of the clutter also influences the probability of detection of the ANMF.

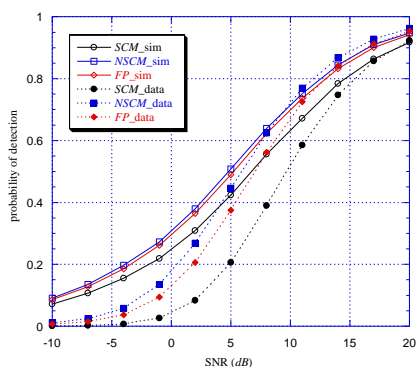
Slide 193  
of 198



## Performance comparison



$N=8, K=16, P_{FA0}=10^{-3} \quad f_D=0, \text{VV data}$



The impact of the non-stationarity is increasingly stronger with decreasing  $P_{FA}$ .

Slide 194  
of 198



## Acknowledgements

- Fulvio Gini, University of Pisa, Italy
- Alfonso Farina, SELEX ES, Rome, Italy
- Jim Sangston, GTRI, Atlanta, USA
- Stefano Fortunati, University of Pisa, Italy
- Pietro Stinco, University of Pisa, Italy

Slide 195  
of 198



## References

- [Aub12] A. Aubry, A. De Maio, L. Pallotta, A. Farina, "Maximum Likelihood Estimation of a Structured Covariance Matrix with a Condition Number Constraint", IEEE Trans. on SP, Vol. 60, No. 6, pp. 3004-3021, 2012.
- [Bak91] Baker C.J., "K-distributed coherent sea clutter," IEE Proceedings-F, Vol. 138, No. 2, pp. 89-92, April 1991.
- [Con87] Conte E., Longo M., "Characterisation of radar clutter as a spherically invariant random process," IEE Proceedings-F, Vol. 134, No. 2, pp. 191-197, April 1987
- [Con96] E. Conte, M. Lops, G. Ricci, "Adaptive matched filter detection in spherically invariant noise ", IEEE Signal Processing Letters, Vol. 3, No. 8, pp. 248-250, 1996.
- [Con98] Conte E., Lops M., Ricci G., "Adaptive detection schemes in compound-Gaussian clutter," IEEE Trans. on Aerospace and Electronic Systems, vol. 34, No. 4, pp. 1058-1069, October 1998
- [Con02a] E. Conte, A. De Maio, and G. Ricci, "Covariance matrix estimation for adaptive CFAR detection in compound-Gaussian clutter," IEEE Trans.-AES, vol. 38, no. 2, pp. 415-426, April 2002.
- [Con02b] E. Conte, A. De Maio, and G. Ricci, "Recursive estimation of the covariance matrix of a compound-Gaussian process and its application to adaptive CFAR detection," IEEE Trans. on SP, vol. 50, no. 8, pp. 1908-1915, Aug. 2002.
- [Far97] Farina, A., Gini, F., Greco, M., and Verrazzani, L., "High Resolution Sea Clutter Data: A Statistical Analysis of Recorded Live Data," IEE Proceedings Part-F, vol. 144, No. 3, pp. 121-130, June 1997.
- [Gin95] Gini F., Greco M., Verrazzani L., "Detection problem in mixed clutter environment as a Gaussian problem by adaptive pre-processing," Electronics Letters, vol. 31, No. 14, pp. 1189-1190, July 1995.
- [Gin98] Gini, F.; Greco, M.; Farina, A.; Lombardo, P.; "Optimum and mismatched detection against K-distributed plus Gaussian clutter," IEEE Transactions on Aerospace and Electronic Systems, Volume: 34 , Issue: 3, 1998, Pages: 860 - 876.
- [Gin99a] F. Gini and J. H. Michels, "Performance Analysis of Two Covariance Matrix Estimators in Compound-Gaussian Clutter," IEE Proceedings Radar, Sonar and Navigation, vol. 146, No. 3, pp. 133-140, June 1999.

Slide 196  
of 198



## References

- [Gin99b] F. Gini and M. Greco, "A Suboptimum Approach to Adaptive Coherent radar Detection in Compound-Gaussian Clutter," IEEE Trans. on AES, vol. 35, No. 3, pp. 1095-1104, July 1999.
- [Gin99c] Gini, F., Greco, M., and Farina, A., "Clairvoyant and Adaptive Signal Detection in Non-Gaussian Clutter: a Data-Dependent Threshold Interpretation," IEEE Trans. on Signal Processing, vol. 47, No. 6, pp. 1522-1531, June 1999
- [Gin00] F. Gini, "Performance Analysis of Two Structured Covariance Matrix Estimators in Compound-Gaussian Clutter," Signal Processing, vol. 80, No. 2, pp. 365-371, February 2000.
- [Gin02a] F. Gini, A. Farina, "Vector subspace detection in compound-Gaussian clutter. Part I: survey and new results," IEEE Trans. on AES, Vol. 38, No. 4, pp. 1295-1311, 2002.
- [Gin02b] F. Gini, M. Greco, "Covariance Matrix Estimation for CFAR Detection in Correlated non-Gaussian Clutter," Signal Processing, December 2002.
- [Gre04] Greco, M., Bordoni, F., and Gini, F., "X-band Sea Clutter Non-Stationarity: The Influence of Long Waves," IEEE Journal of Oceanic Engineering, Vol.29, No.2, pp.259-283, April 2004.
- [Gre09] Greco, M., Stinco, P., and Gini, F., Rangaswamy, M., "Impact of sea clutter non-stationarity on disturbance matrix estimate and detector CFAR", IEEE Trans. on Aerospace and Electronic Systems. Accepted for publication in May 2009.
- [Gre13] M. Greco, F. Gini, "Cramér-Rao Lower Bounds on Covariance Matrix for Complex Elliptically Symmetric distributions ", IEEE Trans. on SP, Vol. 61, No.24, December 2013, pp. 6401-6409.
- [Gre14] M.Greco S.Fortunati, F.Gini, "Maximum Likelihood Covariance Matrix Estimation for Complex Elliptically Symmetric Distributions under Mismatched Condition", Signal Processing Elsevier, in press.
- [Jak76] Jakeman, E., Pusey, P.N., "A model for non-Rayleigh sea echo," IEEE Trans. on Antennas and Propagation, vol. 24, pp. 806-814, 1976.
- [Ken91] J. T. Kent and D. E. Tyler, "Redescending M-estimates of multivariate location and scatter," Ann. Statist., vol. 19, no. 4, pp. 2102-2119, 1991.
- [Mar76] R. A. Maronna, "Robust M-estimators of multivariate location and scatter," Ann. Statist., vol. 5, no. 1, pp. 51-67, 1976.
- [Noh91] T.J. Nohara, S. Haykin, "Canadian east Coast radar trails and the K-distribution" /IEE Proceeding-F/, Vol. 138, No. 2, pp. 80-88, April 1991.
- [Ozt96] Ozturk, A.; Chakravarthi, P.R.; Weiner, D.D.; "On determining the radar threshold for non-Gaussian processes from experimental data." IEEE Transactions on Information Theory, Vol. 42 , No. 4, 1996. Pages: 1310-1316.
- [Ran93] Rangaswamy, M., Weiner D.D., Ozturk A., "Non-Gaussian vector identification using spherically invariant random processes," IEEE Trans. on Aerospace and Electronic Systems, vol. 29, No. 1, pp. 111-124, January 1993.

Slide 197  
of 198



## References

- [Oll11] E. Ollila, J. Eriksson, and V. Koivunen, "Complex elliptically symmetric random variables - Generation, characterization, and circularity tests," IEEE Trans. Signal Process., vol. 59, no. 1, pp. 58-69, 2011.
- [Oll12a] E. Ollila, D.E. Tyler, V. Koivunen, V.H. Poor, "Complex Elliptically Symmetric Distributions: Survey, New Results and Applications," IEEE Trans. on Signal Processing, Vol. 60, No. 11, pp.5597-5625, 2012.
- [Oll12b] E. Ollila and D. E. Tyler, "Distribution-free detection under complex elliptically symmetric clutter distribution," in Proc. IEEE Sensor Array Multichannel Signal Process. Workshop (SAM), Hoboken, NJ, June 17-20, 2012.
- [Pas08] F. Pascal, Y. Chitour, J.-P Ovarlez, P. Forster, P. Larzabal, "Covariance Structure Maximum-Likelihood Estimates in Compound-Gaussian Noise: Existence and Algorithm Analysis", IEEE Trans. on Signal Processing, Vol. 56, No.1, pp. 34-48, 2008.
- [Rich96] C. D. Richmond, " PDF's, confidence regions, and relevant statistics for a class of sample covariance-based array processors IEEE Trans. on Signal Processing, Vol. 44 , No. 7 , pp. 1779 - 1793, 1996.
- [San89] Sangston, K.J. and Gerlach, K., Results on the detection of signals in spherically invariant random noise. Report 9202, Naval Research Laboratory, Nov. 17, 1989.
- [San99] K. J. Sangston, F. Gini, M. Greco, and A. Farina, "Structures for radar detection in compound-Gaussian clutter," IEEE Trans. on Aerospace and Electronic Systems, vol. 35, No. 2, pp. 445-458, 1999.
- [San12] K. J. Sangston, F. Gini, M. Greco, "Coherent radar detection in heavy-tailed compound-Gaussian clutter", IEEE Trans. on Aerospace and Electronic Systems, Vol. 42, No.1, pp. 64-77, 2012.
- [Tyl87] D. E. Tyler, "A distribution-free M-estimator of multivariate scatter," Ann. Statist., vol. 15, no. 1, pp. 234-251, 1987.
- [War81] Ward, K.D., "Compound representation of high resolution sea clutter". Electronics Letters, 17, 6 (1981), 561-563.
- [Wat85] Watts, S.; "Radar detection prediction in sea clutter using the compound K-distribution model," IEE Proceedings F Communications, Radar and Signal Processing, Volume: 132 , Issue: 7, 1985, Pages: 613 – 620.
- [Wat87] Watts, S.; "Radar Detection Prediction in K-Distributed Sea Clutter and Thermal Noise," IEEE Transactions on Aerospace and Electronic Systems, Volume: AES-23 , Issue: 1, 1987, Pages: 40-45.
- [Wie12a] A. Wiesel, "Unified Framework to Regularized Covariance Estimation in Scaled Gaussian Models", IEEE Transactions on Signal Processing ,Vol. 60, No.1, pp.29-38, 2012
- [Wie12b] A. Wiesel, "Geodesic Convexity and Covariance Estimation", IEEE Transactions on Signal Processing, Vol. 60, No. 12, pp.6182-6189, 2012
- [Zha12] T. Zhang, A. Wiesel, M. Greco, "Convexity of the Maximum Likelihood Estimator for the Multivariate Generalized Gaussian Distribution", IEEE Transactions on SP, Vol. 71, No. 16, pp. 4141-4148, 2013 .

Slide 198  
of 198